Water Level Fluctuations of Lake Enriquillo and Lake Saumatre in Response to Environmental Changes

A Masters of Engineering Project
Presented to the Faculty of the Graduate School of Cornell University
In Partial Fulfillment of the Requirements for the Degree of Master of Engineering

by
Eva Joelisa Romero Luna
And
Dina Poteau
August 2011

Abstract

The water level of Lake Saumatre in Haiti and Lake Enriquillo in the Dominican Republic has been increasing in a continuous manner for the past 10 years. This increase in volume has caused flooding of roads, cities and agricultural land causing the inhabitants of the area to complain about the current situation and seek help from their respective governments. Both national and international organizations have expressed interest in determining the causes of the continuous growth and from there, coming up with aid plans for the cities and inhabitants of the area.

Various theories haven proposed by national and international organizations, and other technical groups, to explain the growth of the lakes. Among the hypotheses to explain the growth there is 1) Deforestation of the watershed, which would affect the hydrological balance by means of a change in infiltration rates and 2) Regional climate change which would also affected the hydrological balance of the area by either an increase in precipitation or decrease in evaporation rates.

This study analyzed those two main theories to determine whether they are the cause of the growth. First, deforestation was studied by means of remote sensing of the land cover on the years of 1986 and 2010 and analyzing vegetation changes. A Normalized Differential Vegetation Index (NDVI) was also analyzed to validate the land cover change method. It was found that, although there has been some land cover change, the change has not been significant enough to influence major changes in the hydrological balance. A water balance was also done which resulted in a correlated lakes' level increase with precipitation patterns, indicating that the watersheds are highly responsive to precipitation trends.

These are only preliminary results since there are many unknowns in the dynamics of the lakes' systems. The objective of this study was to do a basic analysis of the dynamics of the two watersheds and provide a starting point for a more in depth research.

Acknowledgments

Many people have helped us immensely to complete this project. We would like to thank our advisors, Tammo Steenhuis and Todd Walter for giving us the opportunity to explore a project that is so close to our hearts and cultures. We would like to thank Steve DeGloria in the Crop and Soil Science department for spending many hours with us in an attempt to get familiar with the software needed for some of our analyses. Also, William Philpot, in the Civil and Environmental Engineering department, for providing us extensive help and advice on remote sensing analyses techniques. And as the saying goes, last but not least, we would like to thank our parents, who were located in our respective field sites during the study and gathered much of our required data; without them, many of the analyses here would not have been possible.

Table of Contents

Figures

Tables

1. Introduction

1.1 Introduction

Lake Saumatre and Lake Enriquillo are saline, terminal lakes located in the central plateau of Hispaniola along the border of Haiti and the Dominican Republic (DR). The two lakes are only about 5 km^2 apart at their closest point and are very similar in hydrogeological properties. They are also home to a number of endemic species of birds, reptiles and aquatic fauna (McGinley, 2009).

Over the last ten years water levels have been rising in Haiti's Lake Saumatre and the Dominican Republic's Lake Enriquillo. This has led to flooding in the towns bordering the lakes, flooding of the agricultural lands as well as occasionally blocking access to the main road connecting Haiti and the Dominican Republic. Nearby farmers have lost entire crops to flooding by the brackish water (Caribbean's biggest lake, 2010; Growing Lake, 2010).

Both Haiti and DR are very limited in environmental monitoring data. Little information and data is available about the lakes hydrological cycles so speculative theories and ideas have developed concerning the lakes' rise. The main factors attributed to the growing lakes have been:

- Increased rainfall over the last years.
- Changes in deforestation and groundwater flow (Pimentel, 2011).
- Sedimentation (Growing Lake, 2010; Pierre et al., 2008). Haiti has severe problems with soil erosion along its hill slopes due to widespread clearing of forest cover for agriculture and charcoal production (Lewis, 1985).

1.2 Objectives

Because current fluctuations are now affecting the livelihoods of surrounding communities as well as frequently blocking the main road connecting the two countries, there has been a heightened desire to understand the factors affecting the hydrology of the lakes'. However there are many unknowns in the dynamics of this lake system.

The objective of this project was to do a basic analysis of the dynamics of the two watersheds as a starting point for further research. The previous theories mentioned above were used as a starting point for the study. Specifically,

1) Determining if there has been any significant land cover change or vegetation changes that would account for deforestation, and;
2) Examining the water balance of the lakes' basins in relation to the lakes' fluctuations.

1.3 Study Site

The lakes are located in an arid region of Hispaniola. The area is described as having a semi-arid climate with an average annual precipitation ranging from 300-1000 mm with high evaporative rates (Vlaminck, 1989). There are high temperatures year round ranging from 20 to 36°C. Rainfall is not well distributed across the year. Most of the rain occurs within two wet seasons. May and October are the peak months for rainfall (Vlaminck, 1989). Figure 1 shows the average monthly precipitation at the border between

the two watersheds. The mountain ranges bordering the watersheds are likely to have higher precipitation rates although the northern mountain range is also semi-arid. Most of the water probably originates in the southern mountains and highlands (Woodring et al., 1924). Rainfall may be insufficient to generate appreciable amounts of runoff in the small catchment. Surface water inputs are probably limited to the ephemeral rivers (Pierre et al., 2008). Groundwater may dominate water input to the lakes from the watershed. The springs and streams of the plain are rather small, with most of the available water originating from the mountains of the watershed. Much of the water is lost to infiltration and evaporation along its course in the watershed (Woodring et al., 1924). Lake Saumatre is fed by a number of springs including a large spring called Source Maneville and Source, both to the northeast, as well as Source Trou Caiman north of Trou Caiman, and Source Lagon along the eastern side (Woodring et al., 1924). The springs around Lake Enriquillo feed the lake around 20,000 m^3 per hour, mainly spring Las Marias and Las Barias (Cocco Quezada, 2009).

1.3.1 Lake Saumatre

At about 120 km^2 , Lake Saumatre is the largest lake in Haiti. It is situated in the Cul-de-Sac plain in central Haiti. The plain is of rectangular shape and measures about 30 km from west to east and averages 12 km from north to south. The lake itself stretches about 24 km from its northwest tip to its southeastern tip with a maximum width of about 10 km. It is bounded by an abrupt rise in mountains bordering the north and south of the plain. In the Haitian watershed, elevations reach about 1,500 meters above sea level. To the west side, the plain borders the Baie du Port-au-Prince and Lake Saumatre is located on the eastern border of the plain. The surface of the plain is composed of alluvium washed down from the neighboring mountains. This porous material easily drains water during rain events (Woodring et al., 1924). The mountains bordering the north and south of the watershed area are composed of limestone. Rainwater is also easily drained and circulated through the porous media of these limestone areas (Woodring et al., 1924).

1.3.2. Lake Enriquillo

Lake Enriquillo is located in the Southwestern region of the Dominican Republic. It is the largest lake in the country and in the Caribbean with an average area of 265 km^2; its watershed encompasses about 3500 km^2. As mentioned before, it is a hypersaline lake of marine origin. A unique aspect of the lake is that it lies about 45 m below sea level, making it the lowest point in the Caribbean (Buck et al., 2005). Its salinity also varies 2 to 3 times that of nearby ocean water. The southwest region is a semi-arid tropical zone with mostly dry vegetation. The lake is bounded by two mountain ranges, Sierra de Neyba to the north and Sierra de Bahoruco to the south, with elevations of about 2200 m and 1600 m above sea level, respectively.

Both lakes are closed lakes with no surface outflow. This characteristic of closed basins makes them particularly sensitive to climatic changes (Kalff, 2002). The fluctuations in the lakes' levels should reflect fluctuations in climatic variables such as temperature and rainfall.

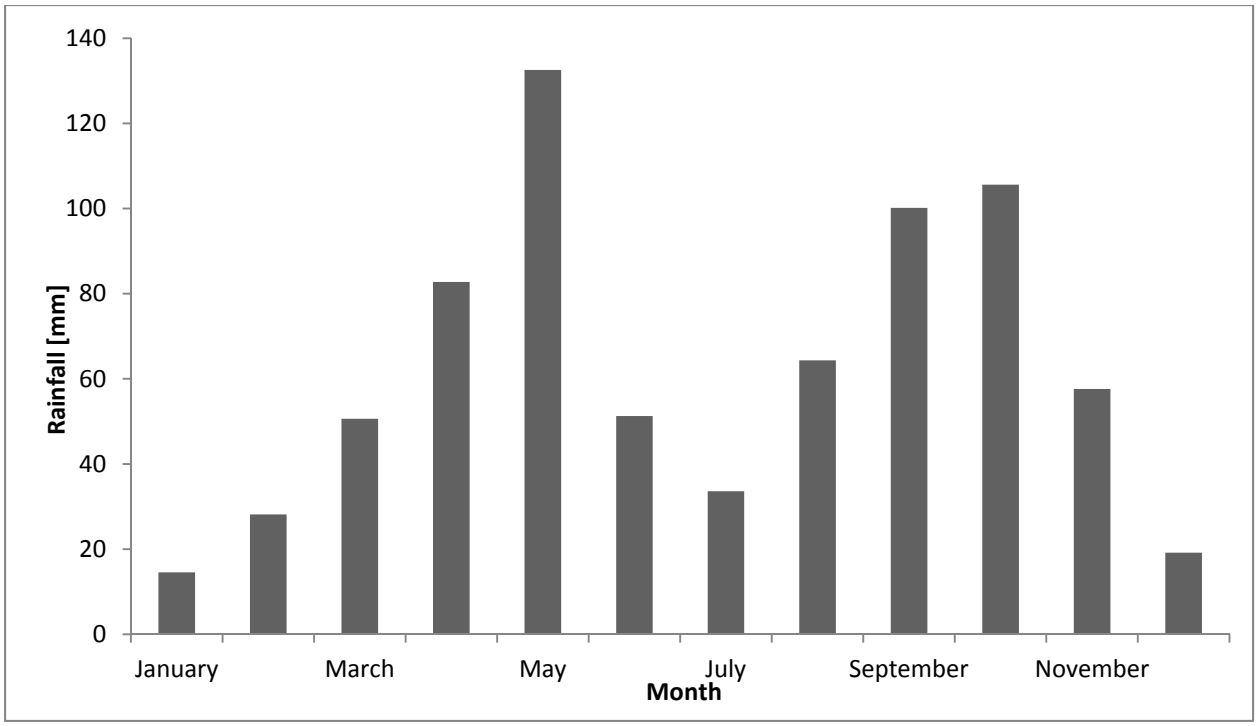

Figure 1.Jimani Station Average Monthly Precipitation.

2. Methodology

2.1 Remote sensing to determine deforestation

Land use and land cover changes can affect the physical, chemical and biological characteristics of the soil. Changes in land use can specifically affect the infiltration capacity: changes from natural or semi-natural vegetation to agriculture or pasture can decrease infiltration rates (Yimer et al., 2008). On the other hand, deforestation or changes from forested land to bare land, would have the opposite effect and the deforested land would have an increase in infiltration rates.

To determine whether the study area has experienced deforestation and, also, whether vegetation changes are related to the lakes' level fluctuations, a land cover/land use change study was done using remote sensing.

Remote sensing is the technique used to extract information from data through image processing and other analyses that allows us to interpret what is on the ground. There are many different procedures that can be used and their usage depends on the user's choice, the quality of the images and the complexity of the analysis.

2.1.1 Imagery Acquisition

The first step in a remote sensing study is to obtain the images that will be processed. There are many satellite sensors to choose from and image characteristics that need to be considered.
Passive sensors, which are sensors that depend on external energy sources such as solar energy, are commonly used for land characterization. These sensors record the intensity of reflected electromagnetic energy at different spectral bands between 400 – 2500 nm.
The key attribute that will influence a sensor's ability to discriminate different cover types include:

1. Spectral resolution: capability of the sensor to distinguish different wavelengths of electromagnetic radiation.
2. Spatial resolution: determined by the pixel size which directly influences the ability to discriminate objects in the horizontal (x,y) dimension.
3. Radiometric resolution: indicates the number of intensity levels that a sensor can use to record radiation.

Current passive optical satellite sensors, with medium spatial resolution, commonly used for land cover mapping include Landsat TM and ETM+ (30 m pixel), SPOT (10 to 20 m pixel), and ASTER (15 to 30 m pixels). Landsat TM and ETM+ imagery were chosen for the study mainly because there were images available dating back to early 1980's which covered the study period. Landsat also had available continuous data that allowed for yearly imagery with similar climate seasons to be used for the study. It orbits the same spot on earth every 16 days (Richard and Jia, 2006).

2.1.2. Data Pre-processing

In order to extract any useful information from remotely sensed images, the raw data obtained by the satellite sensors needed to be pre-processed to correct for distortions that may have occurred due to the remote sensor system characteristics and the environmental conditions. Registration and geometric and radiometric corrections are, usually, the main corrective processes performed. Registration refers to giving correct geographical locations to the pixels in the imagery, radiometric correction refers to correcting the errors induced by the sensor and geometric correction corrects for geometric distortion due to Earth's rotation and other conditions. Landsat TM and ETM+ have the advantage of already being radiometric and geometrically corrected to a first degree and registered.

Other pre-processes performed included resizing and calibrating the data in the images. The Landsat Thematic Mapper (TM) and Enhanced Thematic Mapper Plus (ETM+) acquires temperature data and stores it as a digital number (DN) with a range between 0 and 255. Therefore, the images obtained for the study needed to be calibrated by converting these 8-bit DNs to spectral reflectance by means of equation 1 and 2.

$$\text{Radiance} = \text{Bias} + (\text{Gain} * \text{DN}) \quad (1)$$

$$\text{Reflectance} = \frac{\pi * \text{Radiance} * \text{d}^2}{\text{ESUN} * \cos(\alpha)} \quad (2)$$

Where,
The gain and bias are band specific and are provided along with the image.
D = Earth-sun distance.
ESUN = mean solar exoatmospheric irradiances.
α = solar zenith angle.

2.1.3. Atmospheric correction:

a. Atmospheric scattering:

The energy received by the sensor is a function of incident energy (irradiance), target reflectance, atmospherically scattered energy (path radiance) and atmospheric absorption. Therefore, atmospheric correction and sensor calibration are necessary when multisensory or multi-date images are being classified in order to ensure that pixel values are comparable from one image to the next in a temporal sequence (Richard and Jia, 2006).

Dark object subtraction (DOS) techniques were used to correct for atmospheric effects. DOS consists of subtracting a constant value from all pixels in a given spectral band. DOS is based on the fact that some pixels in the image should have a reflectance of zero and that the values associated with them are effects of atmospheric scattering.
For the images in the study it was assumed that the deepest areas of the lake were dark enough to have a reflectance of zero, therefore, the reflectance shown on those areas was subtracted from all the bands, accounting that the reflectance value measured was haze in the atmosphere.

b. Cloud and Cloud shadow masking:

All the images available for use had some percent of cloud cover. To avoid misclassification of those pixels, cloud pixels need to be removed from the image by creating a mask that will assign a value of 0 to those respective pixels.
Band 1 and, a resampled to 30 meters, band 6, were used to create the mask. Band 1 is the blue band and the clouds appear as the brightest pixels. Band 6 is the thermal band and clouds appear as the darkest pixels since clouds are cold elements. Band math was used within ENVI software to give a value of zero to all pixels between 0-120 in band 1 and from 120 to 255 in band 6. A joined mask was created to neglect all of those pixels.

For the cloud shadow, band math was used to calculate the ratio of band3/band5 and a mask was created from the ratio ranging from 0.7 to 1.2. This cloud shadow interval was determined from visual observation.

The cloud and cloud shadow masks were applied to all images in order to produce an accurate change detection analysis.

2.1.4. Initial Feature Extraction:

When performing image classification, color differences among pixels are the important information that needs to be extracted. To emphasize these differences, different band combinations and band ratios are combined and calculated to determine what works best for visualizing the differences.

The feature extraction technique used for the study was histogram analysis. Histograms show contrast levels and modal characteristics of the data. Histogram analysis along with statistical data helps to determine which bands are and are not highly correlated. The weak correlated bands are used for feature extraction since they contain different information on the observed landscape. Bands 7, 4, 3 corresponding to middle infrared (MIR), near infrared (NIR) and visible were used for the study.

2.1.5. Thematic Information Extraction:

The aim of pattern recognition in the context of remote sensing is to link each object or pixel in the study area to one or more elements of a user-defined label set, so that the radiometric information, contained in the image is converted to thematic information, in this case, land cover classes (Richard and Jia, 2006).

a. Classification System: The following classes (Table 1), obtained from the Dominican Environmental Agency were used for the classification scheme.

b. Classification Process: The classification method chosen for the study was the Maximum Likelihood which is a supervised classification method. Supervised methods rely on the input from the analyst/user and informational classes or types known a priori. With the supervised classification, the identification of representative homogeneous areas or samples of known land cover types is required. Training data sets were selected based on a 7,4,3 band composite and an external land cover map of the Dominican Republic done in 2003 by the Dominican Environmental Agency. Sufficient and representative training data was collected for each class

and scatter plots of different band combinations were analyzed to identify that the training data was indeed represented as a cluster in those band combinations.

The maximum likelihood method is based on the probability of each pixel belonging to each of a predefined set of classes. The pixel is then assigned to the class for which the probability is the highest. The maximum likelihood is based on the Bayesian probability formula:

$$P(x,w) = P(w|x)P(x) = P(x|w)P(w) \quad (3)$$

Where x and w are generally called events. $P(x,w)$is the probability of coexistence (or intersection) of events x and w. $P(x)$ and $P(w)$ are the prior probabilities of events x and w, and $P(w|x)$ is the conditional probability of event x given event w. If x_i is the i^{th} pattern vector and w_j is the information class, then $P(x)$ is the probability of finding a pixel from any class at location x and $P(w)$ is the probability that class w occurs in the image. The probability that x_i belongs to class w_j, or posterior probability, is given by:

$$P(w_j|x_i) = \frac{P(x_i|w_j)P(w_j)}{P(x_i)} \quad (4)$$

	Classification	Description
0	**Unclassified**	Omitted land use/cover in statistics (cloud and cloud shadow cover, non-determined pixels)
1	**Agriculture**	Areas dedicated to food and fiber production. This category includes mixed agriculture, intensive agriculture and pasture.
2	**Shrubs**	Area forested by small, dry trees (i.e.: Guasabara). Small and open vegetated formations adapted to aridity.
3	**Dry Forest**	Area forested by deciduous trees that during the dry season lose their leaves with the function of conserving water.
4	**Coniferous Forest**	Areas forested by trees of conic shaped trunk. The wood is homogenous and forms very clear concentric bands. Generally green year around and leaves are of hard consistency.
5	**Broadleaf Forest**	Areas forested by trees of ramified, well defined, cup. The leaves are of wide category. In its wood concentric bands don't show up as clearly.
6	**Bare Soil**	Areas without vegetated cover or almost non-existent.
7	**Urban area**	Areas of intensive human use and dominated by structures. This category includes cities and towns.
8	**Body of water**	Areas with significant water accumulation.
9	**Sugar Cane**	Agricultural sub-area dedicated to sugar cane production.

Table 1.Classification scheme

2.1.6 Post Classification:

Post classification methods were applied to the obtained classification schemes after all the pixels in the image had been assigned to classes. The classification maps were left with noise of scattered individual pixels in a "salt and pepper" manner. Majority analysis was performed to fix this. Majority analysis consists of changing spurious pixels within a large single class to a specific class.

2.1.7 Classification Accuracy Assessment

Measure of accuracy must accompany any classified map. This allows a degree of confidence to be attached to the results and will serve to indicate whether the analysis' objectives were achieved. To formulate an accuracy assessment, ground truthing points were obtained on a field trip to the study area in May 2011. A thematic map made by the Government Environmental Agency in 2003 was also used for validation of results.

a. Confusion matrix: Accuracy was determined empirically, by selecting a sample of pixels, or testing pixels, from the thematic map and from ground truthing points and checking their labels against classes determined from reference data or ground truth. The percentage of correctly labeled pixels from each class was then calculated along with the proportions of pixels that were erroneously labeled into other classes.

b. Kappa coefficient: The Kappa coefficient, which is calculated from the confusion matrix, was determined by the following relation (Equation 5). If the elements of the error matrix are represented by x_{ij}, the total number of test pixels as P and

$$X_{i+} = \sum_j x_{ij} \text{ (i.e. the sum over all columns for row i)}$$
$$X_{+j} = \sum_i x_{ij} \text{ (i.e. the sum over all rows for column j)}$$

Then the kappa estimate is defined by (Richard and Jia, 2006):

$$\mathrm{K} = \frac{\mathrm{P}\sum_{\mathrm{k}} \mathrm{x}_{\mathrm{kk}} - \sum_{\mathrm{k}} \mathrm{x}_{\mathrm{k+}}\mathrm{x}_{\mathrm{+k}}}{\mathrm{P}^2 - \sum_{\mathrm{k}} \mathrm{x}_{\mathrm{k+}}\mathrm{x}_{\mathrm{+k}}} \quad (5)$$

c. Normalized Differential Vegetation Index (NDVI): An NDVI analysis was done as a validation procedure to confirm that the results of deforestation levels were truly correct. NDVI is a vegetation index, dimensionless and used to indicate the amount of green vegetation present in an image. MODIS imagery from 2000 to 2011 were used for this analysis. The imagery was already processed and calibrated, ready for an NDVI analysis. NDVI is a powerful normalization that forms the basis for most current indices. It is obtained by dividing the difference index by the sum of the near infrared and red reflectance (equation 6):

$$\mathrm{NDVI} = \frac{\rho_{NIR} - \rho_R}{\rho_{NIR} + \rho_R} \quad (6)$$

This index scales between -1 and 1.

2.2. Water Balance

Using available monthly precipitation and long term pan evaporation, a simple Thornthwaite-Mather type water balance model was applied to the two watersheds to simulate water level changes. The water balance used lumped sums of precipitation, and evaporation on a monthly time step. Using the model, rough estimates of the input and outputs components of the lakes' water balances were simulated to analyze their sensitivity to precipitation changes.

The model used is based on methods following procedures in papers by Steenhuis et al. (2009), Steenhuis and van der Molen (1986) and Thorthwaite and Mather (1957). Water balance calculations were performed for two zones of differing infiltration properties. The flat plains and degraded hillslope areas of the watershed were assumed to quickly saturate and generate overland runoff. Conversely, the hillslopes areas have high infiltration rates. Excess rainwater after saturation of the soil column in the hillslopes percolates to a base flow reservoir from which base flow is released to the lakes. It was assumed that runoff and base flow are at the lakes within each time step and parameters do not change over time.

Water balance calculations were made based on monthly time series based mostly on equations from Steenhuis et al. (2009). During months when rainfall leads to a saturated surface soil column, water from the watershed is released into the lakes. Soil storage, S_t, is calculated by equation 7. When S_t reaches the maximum soil water capacity, S_{max}, surface runoff is generated in the low infiltration zone and percolation of the excess water occurs in the high infiltration zone. Runoff and percolation are calculated from equation 8 and 9. Base flow from percolated water is released from a subsurface reservoir that behaves as a linear reservoir following equations 11-13.

$$S_t = S_{t-1} + (P - AET - R - Perc) \quad (7)$$

$$R = Perc = S_{t-1} + (P - AET) \quad if\ S_t = S_{max} \quad (8)$$

$$R = Perc = 0 \quad if\ S_t < S_{max} \quad (9)$$

$$E = pan * E_p \quad (10)$$

$$S_{bf,t} = S_{bf,t-1} + Perc - Q_{bf,t-1} \quad if\ S_{bf,t} < S_{max} \quad (11)$$

$$Q_{bf,t} = S_{bf,t} * (1 - e^{\left(\frac{0.69}{t_{1/2}}\right)}) \quad if\ S_{bf,t} < S_{max} \quad (12)$$

$$Q_{bf,t} = S_{max} \quad if\ S_{bf,t} = S_{max} \quad (13)$$

When precipitation is greater than evaporation over the monthly time step, excess rainwater either directly generates surface runoff or recharges subsurface base flow reservoir. When the maximum reservoir storage is set to 90 mm or greater, the reservoir never reaches capacity. Based on the assumption that the base flow reservoir fills first and the storage reservoir never reaches capacity under the semi-arid conditions, no calculations were made considering interflow or flow dynamics once the reservoir fills.

$$if\ P - E > 0\ then,$$

$$S_t = P - E + S_t - 1 \quad (14)$$

$$AET = PET \quad (15)$$

When evaporative rates exceed precipitation over the monthly time step, water from storage depletes.

$$if\ P - E < 0\ then,$$

$$S_t = S_{t-1} * e^{[(P-E)/S_{max}]} \quad (16)$$

$$AET = e^{(S_t/S_{max})} \quad (17)$$

(Steenhuis and van der Molen, 1986)

The model calculations output estimates for runoff from the surface, R, percolation, Perc, base flow, Q_{bf}, base flow storage, S_{bf}, maximum soil storage, S_{max}, actual evapotranspiration, AET, and potential evapotranspiration, E. The parameters used are the accumulation of rainfall during each month, P, monthly long-term pan evaporation, E_p, a pan factor, "pan", and reservoir half-life in months, $t_{1/2.}$

Once amount of water coming from the watersheds has been calculated, the potential change in the lakes' storage is determined from a mass balance of watershed inputs, lakes' evaporation and precipitation directly over the lakes.

$$Change\ in\ storage = watershed\ input + precipitation\ over\ lake - lake\ evaporation$$

$$\Delta V = (WS) * (A_{watershed}) + (P) * (A_{Lake}) - (E_{pan}) * (A_{Lake}) \quad (18)$$

$$Change\ in\ Elevation = (Change\ in\ Storage) / (Lake\ Area)$$

$$\Delta H = \frac{\Delta V}{A_{Lake}} \quad (19)$$

$$WS = R + Q_{bf} \quad (20)$$

Where,

$A_{Watershed}$: Area of the watershed,

A_{lake}: Area of the lake,

ΔV: Change in storage,

ΔH: Change in lake elevation.

2.3 Water Balance Data

2.3.1. Climate Data

Monthly precipitation data from two stations were used for the water budget calculations of the Lake Saumatre and Lake Enriquillo basin. One station is located in the town of Jimani in the Dominican Republic. It is about 2 kilometers south of the southeastern corner of Lake Saumatre near the edge of the watersheds. The second station is located in Damien, Haiti. It is about 19 kilometers west of the watershed and 23 kilometers west of the lake. These two stations were the nearest stations available with continuous data over the past 30 years. There were two months from the Jimani station data with missing data values: November 2004 and December 2004. Due to the scarcity of nearby station data for the dates of interest, the two months in questions were filled with values from the Damien stations. The two dates with missing data occur during the dry season when precipitation is minimal. It is unlikely that

soil would reach saturation during these months. The values substituted from the Damien station should not have significantly effected calculations. The precipitation data from the Damien station was obtained from the Ministry of Agriculture, Natural Resources and Rural Development (MARDNR) in Haiti and the Jimani station data was obtained from the Department of Climatology in the Dominican Republic.

Thiessen polygons were used to estimate one lumped value of average watershed precipitation for the Lake Saumatre basin. Rainfall for each month was calculated as the sum of the percent areas of the Thiessen polygons for a rainfall station multiplied by the sum of rainfall for a given month. The areas of the Thiessen polygons of the location of the point stations are illustrated below in Figure 2.

$\mathrm{P_{gross}} = \text{net precipitation calculated from Thiessen polygon method}$

$$P_{gross} = \sum(\pi * (\%AreaCovered_j)) \tag{21}$$

$\mathrm{E_{pan}} = \text{Long term evaporation}$

$$E_{pan} = (pan\ evaporation) * (pan\ coefficient) \tag{22}$$

The pan evaporation data is from a site in southeastern Puerto Rico. The location in Puerto Rico is a semi-arid region at an average elevation of 27 m (Harmsen et. al, 2004).

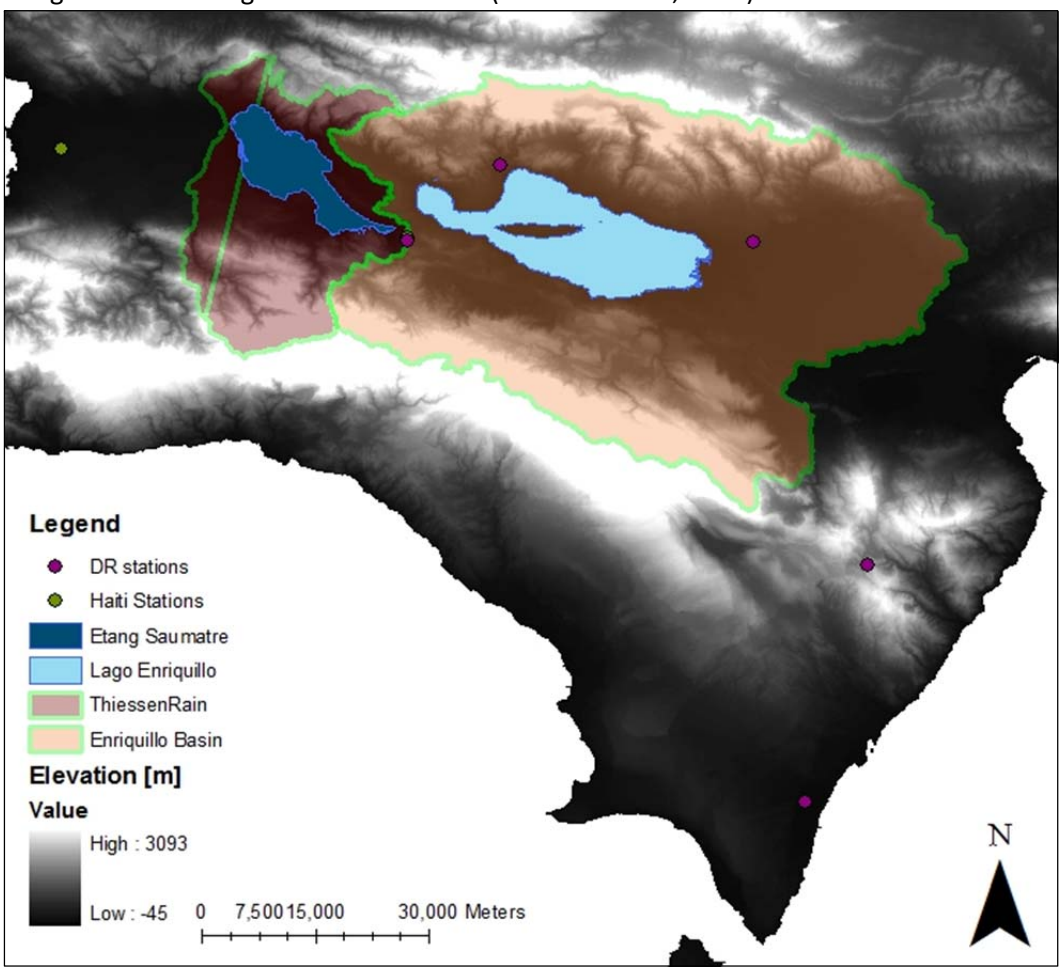

Figure 2.Rainfall Stations and Watershed Areas of Lake Saumatre and Lake Enriquillo as well as the Thiessen Polygon areas of the Lake Saumatre.

2.3.2. Water Capacity of Soil

A small soil survey done in 2004 by the USAID (Guthrie and Shannon, 2004) was used to provide initial values and a range of possible water capacity values. Study sites in Saint Georges, Bergeau and Titanyen represented Haitian lowlands with basaltic and limestone soils. These soils have water capacities ranging from about 37 to 74 mm. Sites in Fort Jacques and Salagnac were selected to represent mid to highland soils with soil water capacities ranging from about 120 mm to 250 mm. The coordinates for the locations of the study sites indicated can be found in the appendix (Table 6.4).

2.4 Watershed Delineation

The Lake Saumatre and Lake Enriquillo watersheds were delineated with the use of the ArcHydro and the ArcSWAT extension of ArcMap. A DEM from Hydrosheds program of the USGS and a batch polygon of the lakes' areas were used as input.

2.5 Lake Area Calculations

Area changes due to water level rise are initially minimal in the lakes due to steep surrounding slopes. An attempt to more accurately delineate the lakes' area was done by using thresholds of the near infrared band in a subset of the lakes' area from satellite imagery. Because near infrared radiation is strongly absorbed by water, it appears darker than other features in the near infrared band. Using this band, water from the lakes was delineated from the surrounding land area. The resulting lakes' areas were used as input in a simulation of storage change with the lake.

2.6 Bathymetric Mapping using a Reflectance Ratio

An attempt was made to derive bathymetry from remote sensing imagery. Bathymetric maps of the lake over time would help provide more information on the storage changes in the lake. Originally, the goal of the bathymetry mapping was to gauge possibility of high rates of sedimentation within the lake but the calibration of the relative bathymetry maps produced depth maps of low accuracy. Despite the low degree of accuracy, the maps produced provide information on lake storage that was utilized in the scaling of the water balance.

The waters of Lake Saumatre are usually clear with a slight greenish-blue tint (McGinley, 2009). These conditions are favorable for color reflectance analysis. It is assumed that there are differing types of sediment input at varying locations around the lake. This implies that composition of the bottom of the lake must be taken as variable. Spatially variable bottom reflectance is a source of error in calculations when using visible band imagery. Ratio measurements from two bands can minimize these bottom effects. Another challenge in using reflectance data is the depth of the lake. It is estimated that Lake Saumatre is about 20-24 meters at its deepest point (Pierre et al., 2008; Matthes, 1988). At this depth, calculations using reflectance data may become imprecise. The limit of depth detection is about 20 to 30 using a blue band but these techniques are usually only reasonably precise for depths up to about 12m (Gao, 2009). To overcome this obstacle, the coastal or littoral area of the lake will be examined for sediment accumulation.

2.6.1. Reflectance Ratio

A reflectance ratio of measurements from differing spectral bands can provide information on water depth. The reflectance ratio is based on the varying absorptivity of water between spectra bands. The irradiance reflected from higher absorptivity bands decreases more quickly with depth than lower absorptivity bands. This property is used to formulate a ratio relating two spectra to a constant factor (Stumpf et. al, 2003). This constant factor scales the ratio to depth with the following relationship in equation 23:

$$Z = m_1 \frac{\ln(nR_w(\lambda_l))}{\ln(nR_w(\lambda_f))} - m_0 \tag{23}$$

The R_w terms are the reflectance values of pixels for the two bands, n is a constant that ensures a linear relationship between the ratio and depth and the m terms are constants that scale the R_w ratio to depth. This method is effective in relatively clear and shallow water depths. The relatively simple equation with only two variables to resolve makes this technique very practical.

2.6.2. Imagery

There are a few sources of multi-spectral imagery available for a ratio analysis including satellite imagery from Landsat, MODIS (Moderate Resolution Imaging Spectroradiometer), ASTER (Advanced Spaceborne Thermal Emission and Reflection Radiometer), or MISR (Multi-angle Imaging Spectroradiometer). Relatively high resolution imagery is needed to capture variations in the bathymetry. Based on the criteria, ASTER imagery and Landsat TM imagery can provide appropriate data for the study. ASTER images have four bands in the visible and near infrared with a 15 m resolution. Landsat offers the benefit of the blue visible band that penetrates through deeper water but at a coarser resolution of 30 by 30 meter pixels. Initially ASTER imagery was used but the available bands in the ASTER imagery poorly correlated with point depth data collected. Due to the limitations of using ASTER imagery, two Landsat TM 5 images were used to create a very coarse map of the depth profile of the lake.

In the absence of appropriate dark objects for atmospheric corrections, the raw data from the images were converted to radiance and then converted from radiance to exoatmopsheric reflectance. The minimum reflectance of the near infrared band over a section of the deepest water in the lake was used

as a reasonably dark object to carry out a dark object subtraction. The near infrared band is almost completely absorbed by the water, so the minimum reflectance value over deep water was taken as a reflection of atmospheric effects.

The lake has secchi disk depths ranging from 2 – 3.5 meters (Vlaminck, 1989). As rule of thumb, passive depth calculations using visible band imagery can be done for 2-3 times the secchi depth of water (Gao, 2009). About 40% of the lake is 5 meters or less and 60 percent is deep water. Using the Landsat imagery, depth was calculated up to 10 meters. Depths over this threshold were assigned as deep water pixels. Relative bathymetry was then calculated using equation 24.

$$Relative\ bathymetry\ = \frac{ln(1000 * B1)}{ln(1000 * B2)} \tag{24}$$

B1 is the blue band reflectance and B2 is the green band reflectance, n is taken to equal 1000 to ensure positive values of the ratio (Stumpf, 2003).

3. Results

3.1 Remote Sensing approach to determine deforestation.

Maximum Likelihood estimator was used to extract the thematic information available from the images. A total of 9 classes with specified classification were produced by using this method for each image. An analysis of digital change detection was used for the study and percentages of change were produced. Figure 3 presents the comparison of land cover statistics between the two study years of 1986 and 2010. Figure 5 and 6 present the generated maps for each study year.

The comparison on Figure 3, between years 1986 and 2010 reveals that some changes have occurred in land cover, but that these changes have been very subtle. Among the occurred changes, it can be observed that urban zones have expanded and that the areas of agriculture have decreased. The forests, especially on the mountain ranges, have remained somewhat constant, at least among the forest category. The total percentage of the bodies of water has also increased. On the maps produced (Figures 5 and 6) it can be seen that not only Lake Enriquillo and Lake Saumatre have increased in volume but also other bodies of water such as Laguna Rincon, south-east of the lakes.

In addition, another study done in order to validate the results obtained from the maps produced, was the Normalized Differential Vegetation Index (NDVI). This analysis shows the green index or an estimation of vegetation cover based on the measurement, with remote sensors, of the intensity of the near infrared radiation in relation to the visible. The values of the index oscillate between -1 and 1. In Figure 7 it can be seen that the NDVI values from year 2000 until 2011 have remained relatively constant with a minimum index of 0.48 in 2000 and a maximum of 0.57 in year 2004. These fluctuating values of NDVI do not correspond to changes in lakes' levels, which show that changes in vegetation and forestation of the area, are not instantaneously affecting the size of the lakes.

Accuracy of results: Using ground truthing points (Figure 4), a confusion matrix was produced and the overall accuracy and Kappa Coefficient were determined. The overall accuracy resulted in 56/72 or 77.7%. The Kappa Coefficient resulted in a value of 71%.

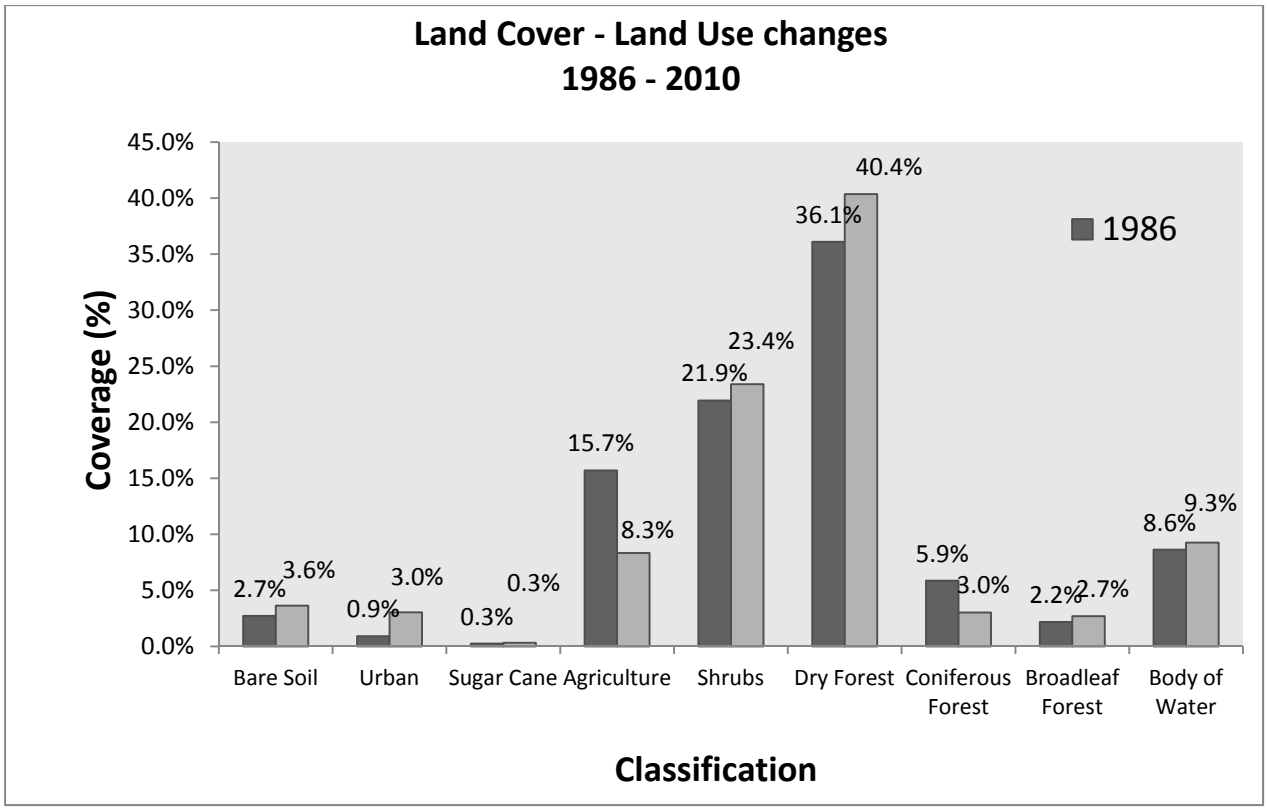

Figure 3: Land Cover and Land Use Changes between 1986 and 2010.

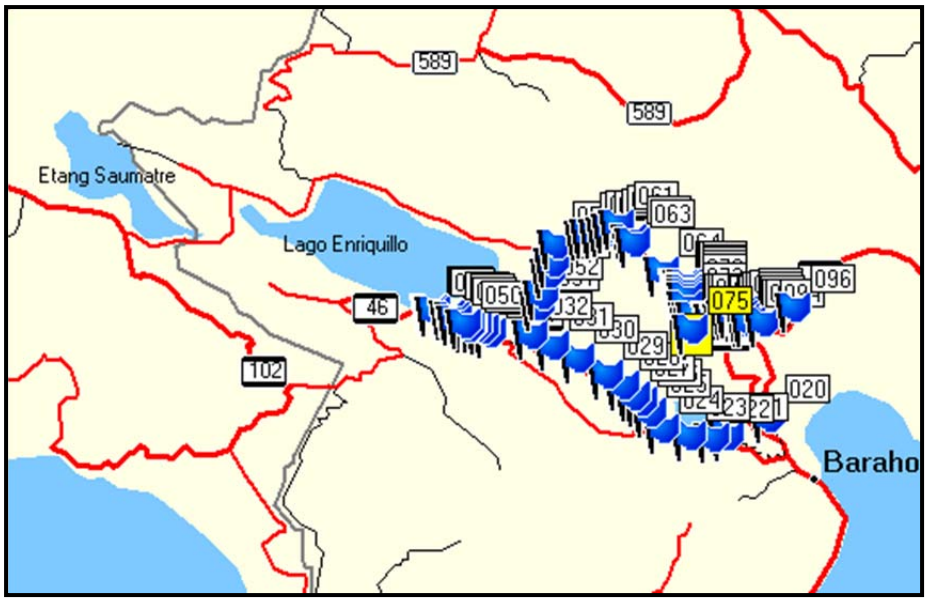

Figure 4. Ground truthing points – Field Trip May 2011.

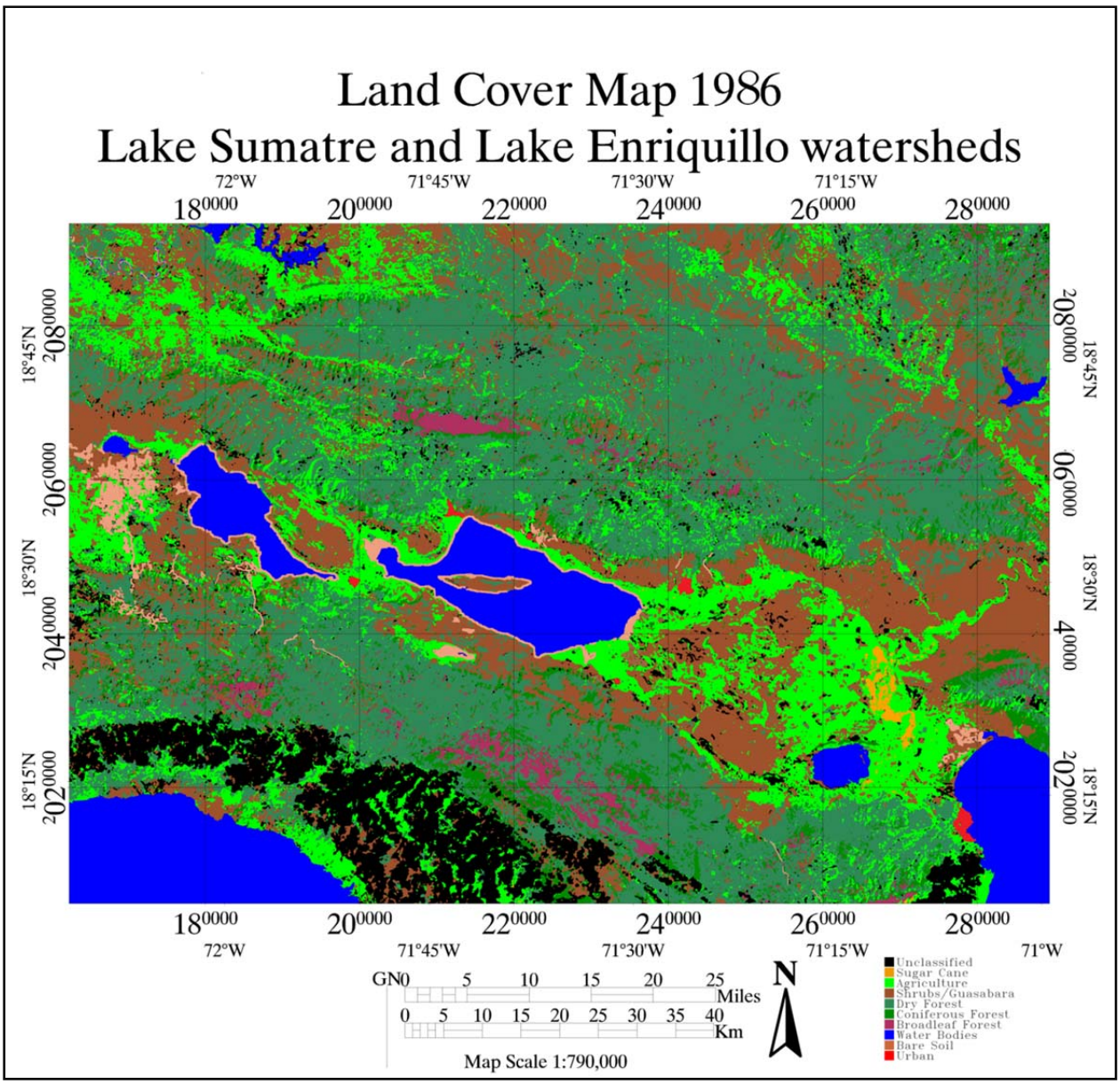

Figure 5: Land Cover map corresponding to year 1986. Lake Saumatre and Lake Enriquillo watersheds.

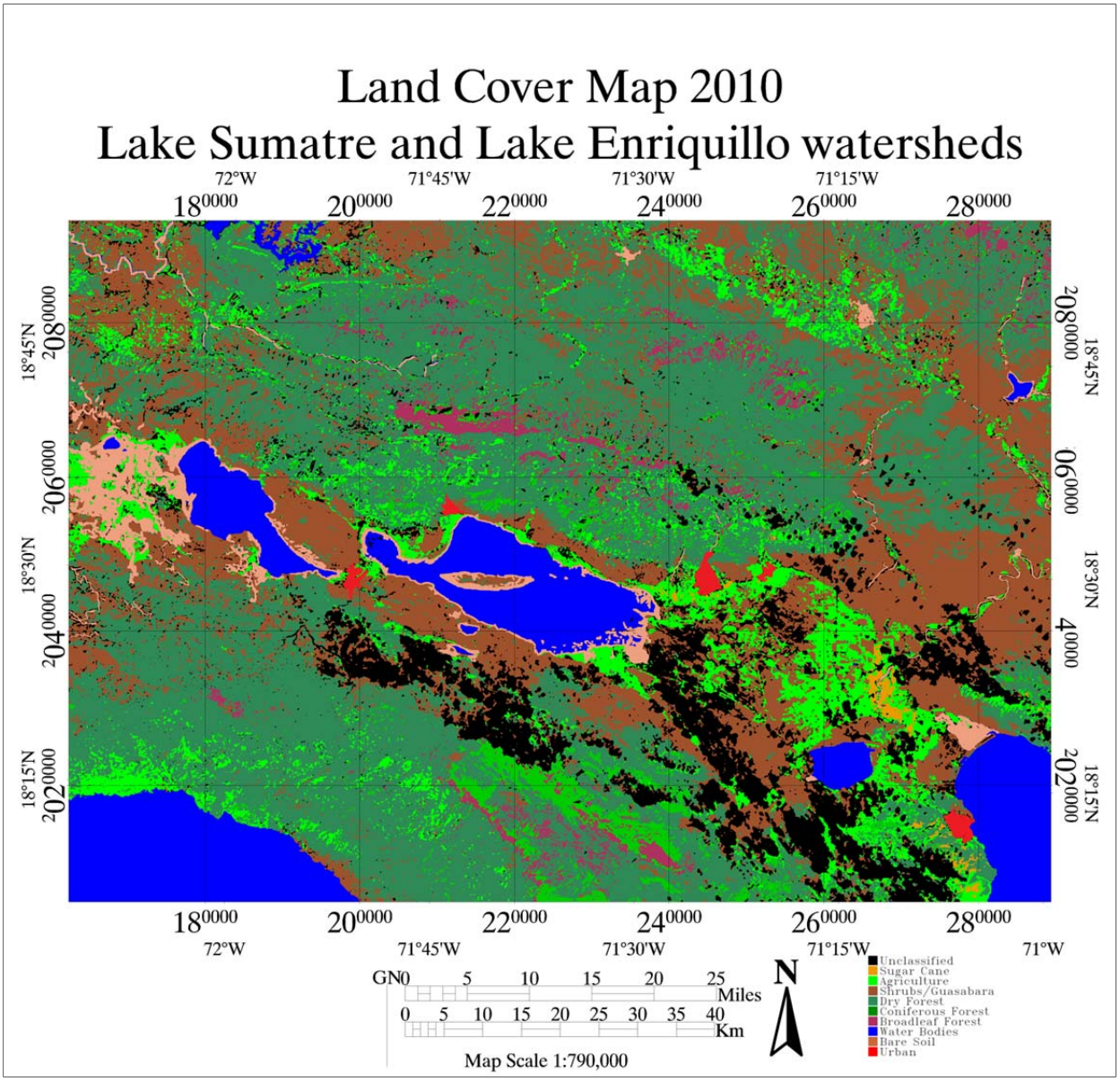

Figure 6. Land Cover map corresponding to year 2010. Lake Saumatre and Lake Enriquillo watersheds.

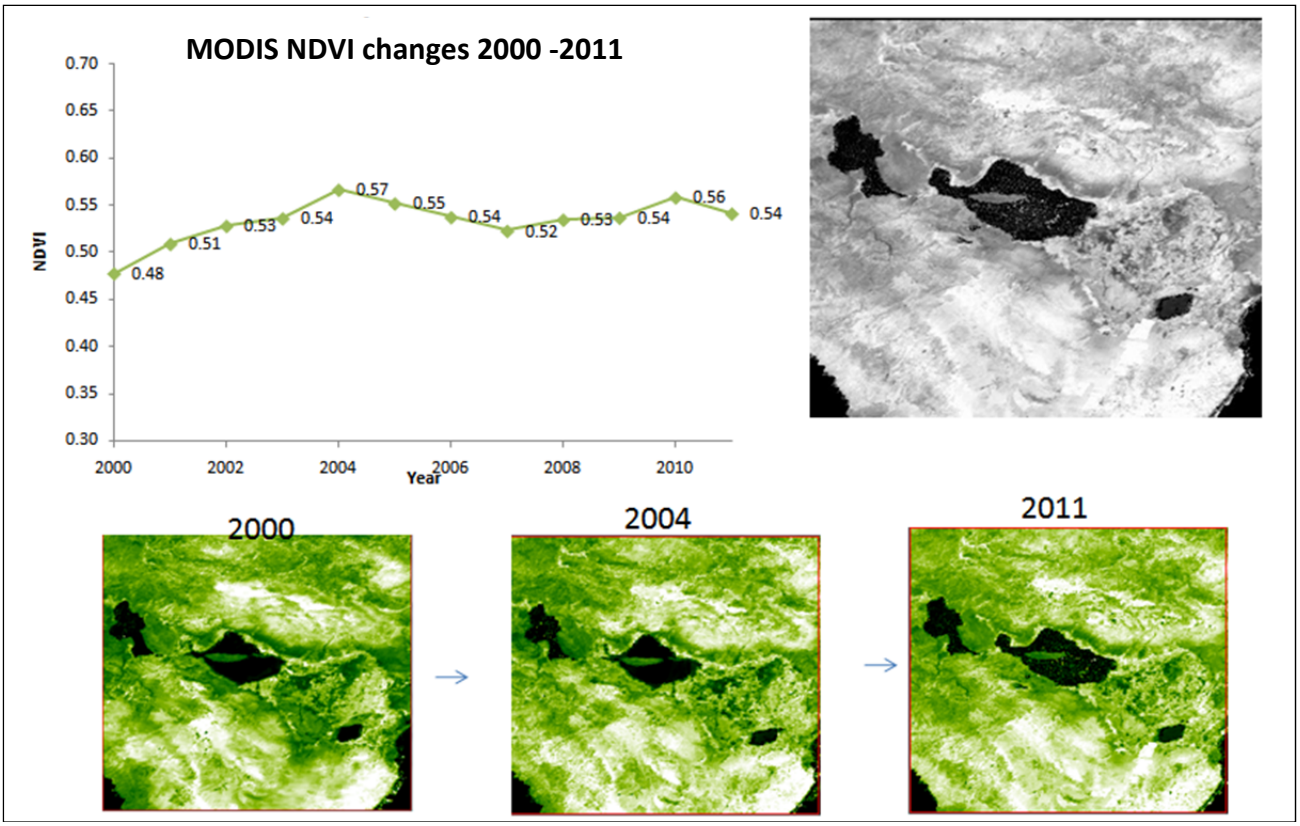

Figure 7: Normalized Differential Vegetation Index (NDVI) 2000 – 2011.

3.2. Bathymetry Map

Depth measurements are needed to scale the reflectance ratios to actual depth. Measurements of depth were made in the southern proportion of lake and used to calibrate the map by deriving the values of m1 and m2 from equation 23. A linear regression of ratio data and several depth measurements made below 40 feet were used to scale the ratio maps to depth. The equations used are found in Table 2 and graphed in Figure 8 below. The resulting depth map of Lake Saumatre is shown in Figure 9.

	R^2	Linear Regression
2011	0.44	400.2x - 402.6

Table 2. Linear Regression of Depth Data for April 2011 Bathymetry Maps.

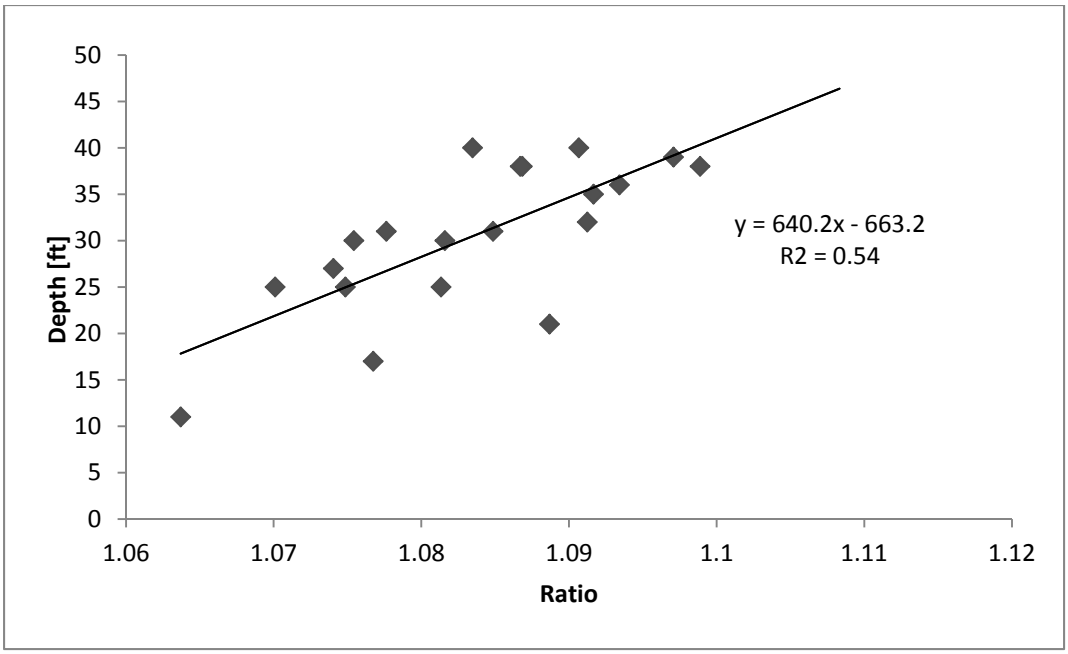

Figure 8.Linear Regression of Depth Data for April 2011 Bathymetry Map.

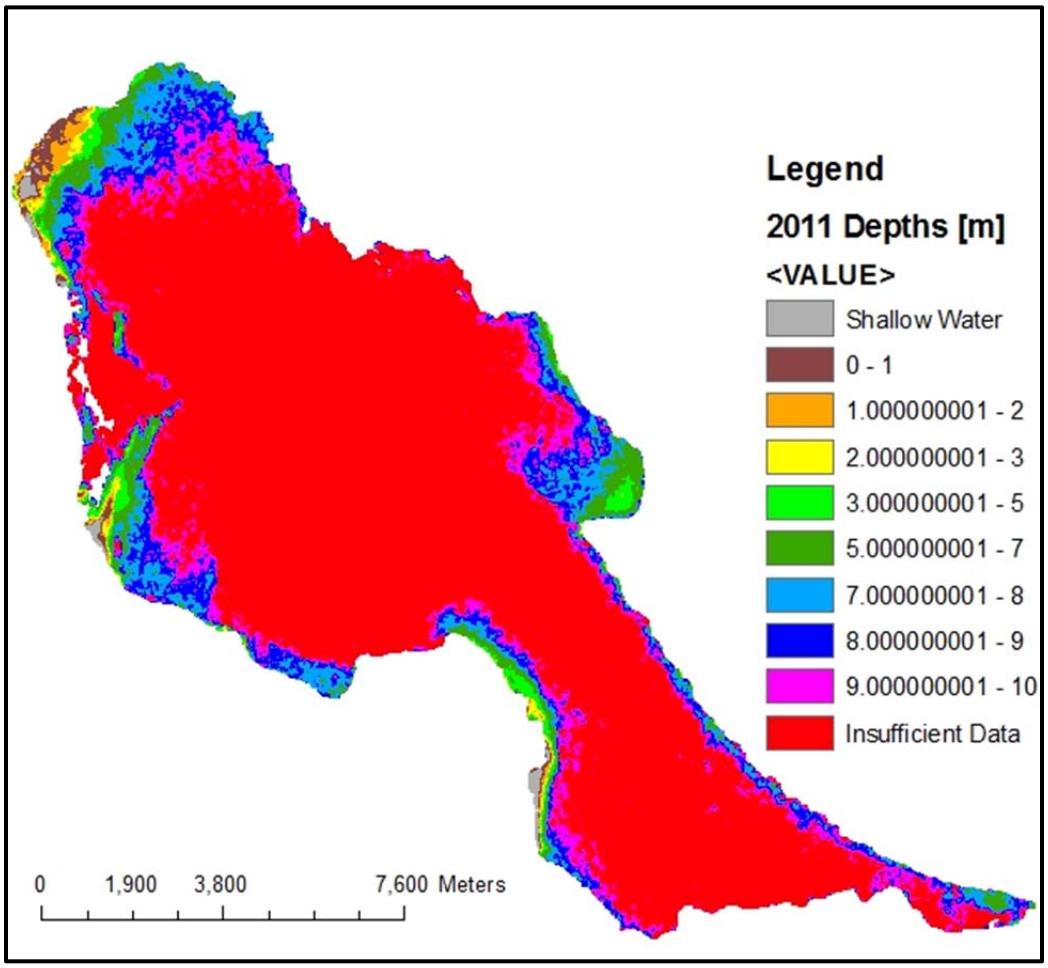

Figure 9. Map of Bathymetry for April 2011.

3.2 Surface Area and Lake Elevation Change

The surface area of the Lake Saumatre fluctuates between 113 to 118 km^2 from 1985 to 2002. The area of Lake Enriquillo fluctuates between 195 to 332 km^2 from 1982 to 2010. After 2003, both lakes experience a clear increasing trend of surface area increase. Surface area of Lake Saumatre has increased about 15% from 1985 levels and Lake Enriquillo has increased 40% from its smallest area in 2003. The surface area of the Lake Saumatre only fluctuated between 113 to 118 km^2 from 1985 to 2002. The area of Lake Enriquillo fluctuated between 195 to 212.3 km^2 from 1982 to 2002. After 2003, both lakes experienced a clear increasing trend of surface area increase with Lake Saumatre reaching an area of 132 km^2 in 2011 and Lake Enriquillo reaching an area of 332.2 km^2 in 2010. In Lake Saumatre ,the larger rate of surface area increase since 2007 may be related to water levels reaching lower sloping areas in the northwestern portion of the lake. Table 3 provides yearly areas of the two lakes. The areas of the two lakes were then related to lake elevation using a linear regression. Elevation data was obtained from the bathymetry map of Haiti and observed lake levels in Lake Enriquillo shown in Figure 10.

LakeSaumatre, Haiti			LakeEnriquillo, D.R.		
Date	Year	Area [km^2]	Date	Year	Area [km^2]
2-Feb-85	1985	115	17-Jan-82	1982	291.6
20-Jan-86	1986	114		1983	
23-Jan-87	1987	113	23-Jan-84	1984	285.1
1-Nov-88	1988	115	2-Feb-85	1985	271.7
4-Jan-89	1989	114	20-Jan-86	1986	268.4
31-Jan-90	1990	114	23-Jan-87	1987	268.3
	1991		1-Nov-88	1988	262.9
22-Feb-92	1992	113	4-Jan-89	1989	262.8
	1993		31-Jan-90	1990	259.7
	1994			1991	
	1995		22-Feb-92	1992	238.2
10-Jul-96	1996	116		1993	
27-Jun-97	1997			1994	
30-Jun-98	1998	113		1995	
1-Jun-99	1999	115	10-Jul-96	1996	225.5
6-Aug-00	2000	116	27-Jun-97	1997	212.5
29-Jan-01	2001	118	30-Jun-98	1998	197.9
9-Feb-02	2002	117	1-Jun-99	1999	231.2
12-Feb-03	2003	116	6-Aug-00	2000	232.4
1-Jun-04	2004	117	29-Jan-01	2001	233
	2005		9-Feb-02	2002	212.3
1-Dec-06	2006	118	12-Feb-03	2003	194.9
11-Aug-07	2007	119	30-Jan-04	2004	198.6
1-Sep-08	2008	124	16-Jan-05	2005	202.5
1-Mar-09	2009	127	3-Jan-06	2006	236.4
22-Jan-10	2010	129	22-Jan-07	2007	255.9
10-Feb-11	2011	132	9-Jan-08	2008	303.2
			11-Jan-09	2009	331.6
			22-Jan-10	2010	332.3

Table 3. Time Series of Lake Area Change for Lake Saumatre and Lake Enriquillo.

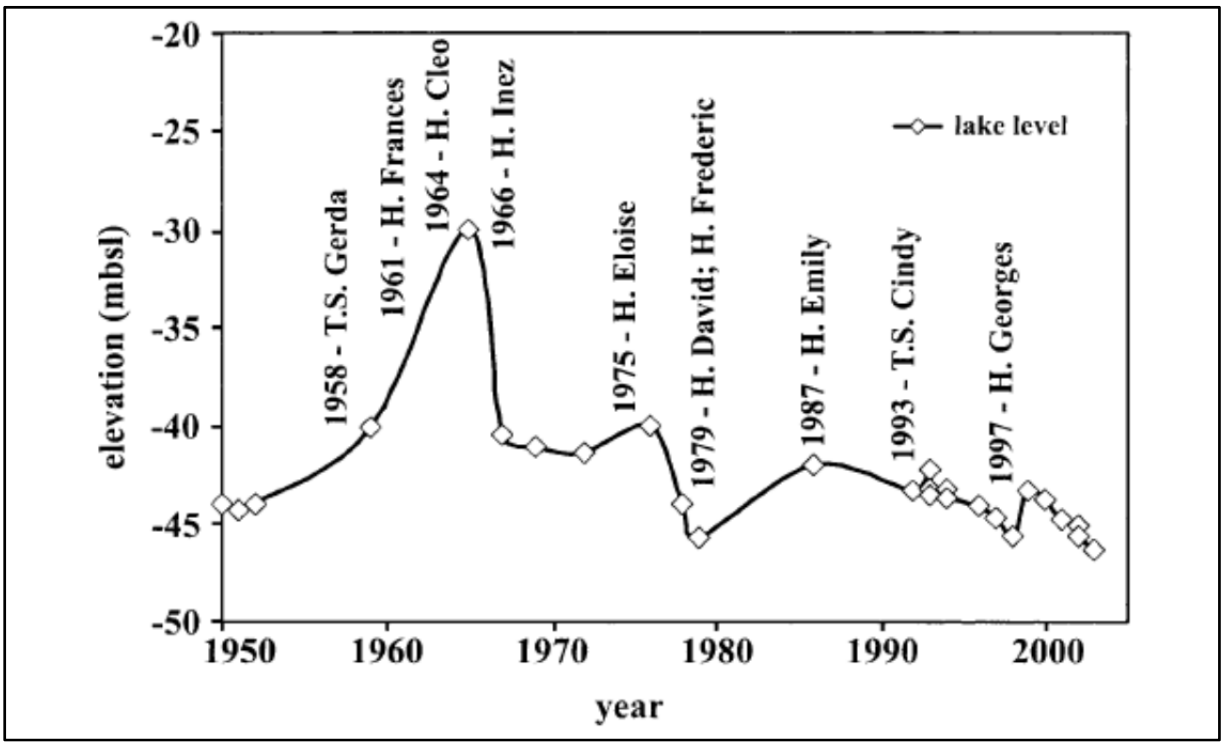

Figure 10. Elevations of Lake Enriquillo in meters below sea level (mbsl) from 1950 to 1963, and the timing of hurricanes (H.) and tropical storms (T.S.) passing near the Enriquillo basin. (Buck et al. 2005).

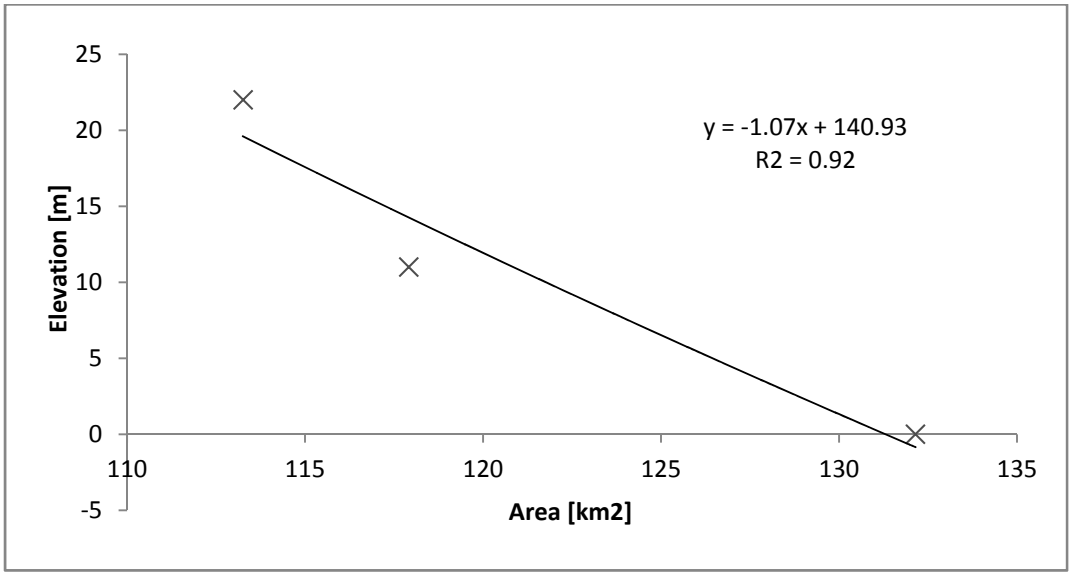

Figure 11. Elevation Interpolation – Area vs. Elevation: Lake Saumatre.

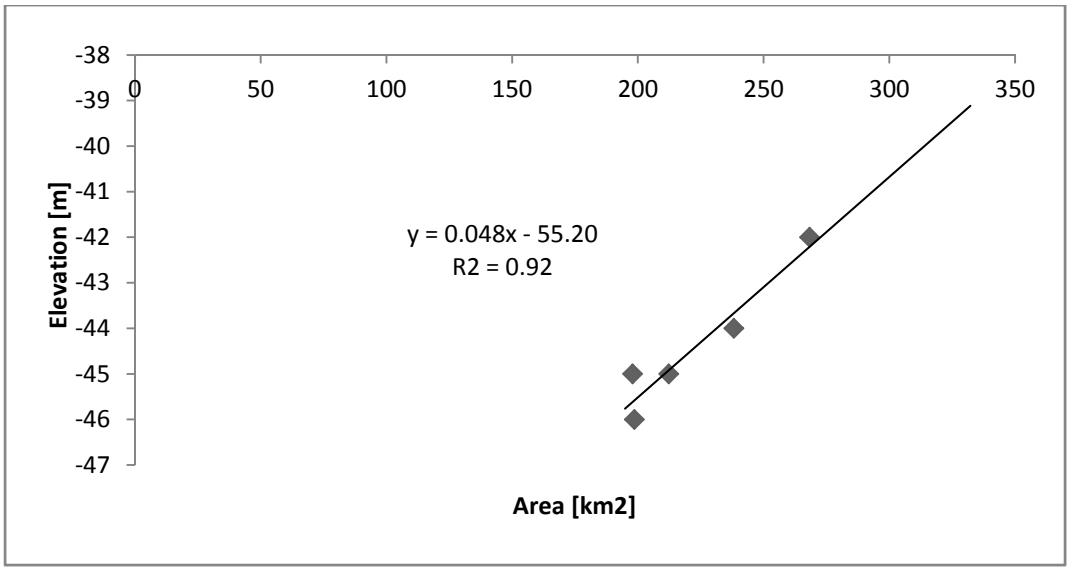

Figure 12. Elevation Interpolation - Area vs. Elevation: Lake Enriquillo.

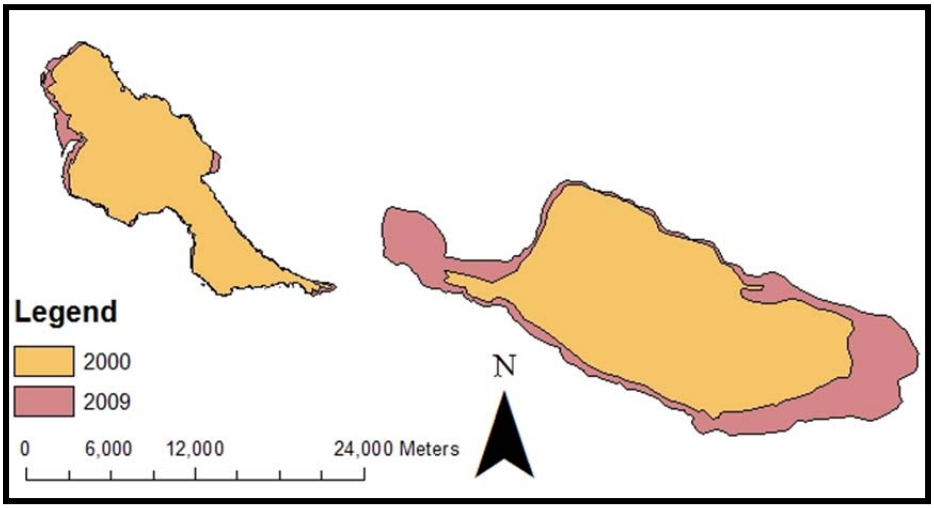

Figure 13. Map of Lake Area Change. Lake Saumatre on the left and Lake Enriquillo on the right.

3.3. Water Balance

The water balance model used only considered variations in precipitation as a factor in lake level change. Other factors such as temperature, radiation and land use change can also cause significant changes to lake storage. By only considering precipitation, it is possible to determine whether, precipitation can sufficiently explain lake level change patterns.

Lakes Saumatre and Enriquillo are hydrologically closed basin lakes therefore only two sources of inputs of precipitation and watershed inputs and one output of evaporation mainly control lake level changes. Evaporation is the sole water output used in the model. The lake balance was very sensitive to evaporation. The shape and magnitude of the resulting lake level simulation was highly dependent on the evaporation coefficient. Although, it appears important to correctly represent evaporation, obtaining evaporation rates is difficult. Due to the lack of environmental data, it was not possible to derive evaporation nor were local pan evaporation measurements available. Long term evaporation rates from a Puerto Rico site were used for evaporation estimates. The long term values provide basic estimates but cannot capture interannual variations in evaporation. This limitation may be a significant source of error in the water balance calculations.

There is also a high degree of uncertainty relating the magnitude of the storage capacities of soil used. All parameters were manually adjusted to fit the simulated lake level to the lake levels derived from lake area. To create this fit, soil capacities in the lower range of the values from USAID survey (Table 6.4) were used in the Dominican lake's water balance. It had to be assumed that the Haitian watershed's soils had very low water capacities in all areas of the watershed, to create a simulation curve of similar shape to the derived lake levels in the Lake Saumatre. It is assumed that 55% of the watershed area quickly generates surface runoff from rain events with a soil capacity of 25 mm. This area is a combination of degraded hillsides and the valley. The remaining hillslope areas are also modeled as having low storage capacities of 70 mm. The need to adjust the soil capacity to these values for the model may correspond to the degraded nature of the severely deforested and eroded Haiti landscape. Alternatively, the low soil storage may indicate the need to include another significant hydrological variable into the model to adequately derive the lake level patterns.

All the final parameter values used are shown in Table 4 including the soil water capacities, the portions of infiltration zones, pan coefficients and aquifer half-lives. Figure 14 and 15 display the main water inputs and outputs including direct rainfall, evaporation, and watershed inputs. Watershed inputs was a combined value of the runoff and base flow from the watershed. Surface runoff accounted for 60% of the water from the catchment and subsurface flow accounted for 40% of the flow. Figures 16 and 17 show simulated lake levels overlaid by the yearly elevation change. As shown, the monthly water balance simulation moderately fits the elevation changes.

The lake elevations in the graph are plotted in terms of change from the lowest level. For Lake Saumatre, a lake level of zero is plotted for 1998, the year of the lowest lake surface area. Elevations in Lake Saumatre varied within a range of about 1.5 m from 1985 to 2002. After 2003, Lake Saumatre had a rapid rise of about 5 m in water levels over just 8 years. While following the general pattern of lake rise, after 2003, the modeled lake levels overestimate elevation estimates by 0.5 to 3 m.

The lowest surface area for Lake Enriquillo occurs in 2003. Before 2003, Lake Enriquillo varied within a range of about 4.5 m from 1982 to 2002. Within 7 years after 2003, Lake Enriquillo made a rapid rise of about 6.5 m.

The result of the water balance simulation illustrates rainfall exceeding a threshold in terms of soil capacity in 2003. In the last 7 to 8 years, there has been an increase in months of high precipitation leading to high watershed inputs. Excess water after soil saturation began to surpass evaporative losses. Increases in water proceeded the increase in storage of the lakes. In 2009, calculated water inputs generated from the watershed began to level off. Lake levels would be expected to follow a similar trend, but from 2009 to 2011 the lake area of Lake Saumatre has continued to increase at a high rate. This could indicate another factor involved in the lake level rise or the area increase could be due to the water surface reaching lower sloping areas.

Lake Enriquillo, D.R.			**Lake Saumatre, Haiti**		
	Area (Portion)	Storage (S_{max}) [mm]		Area (Portion)	Storage (S_{max}) [mm]
Saturated Area	0.1	40	Saturated Area	0.2	25
Degraded Hillslope Area	0.2	40	Degraded Hillslope Area	0.35	25
Hillside – Recharge Area	0.7	150	Hillside – Recharge Area	0.45	70
Pan Factor		0.89	Pan Factor		0.86
Aquifer Half-life		10 days	Aquifer Half-life		10 days

Table 4. Parameters Used in Water Balance Calculations.

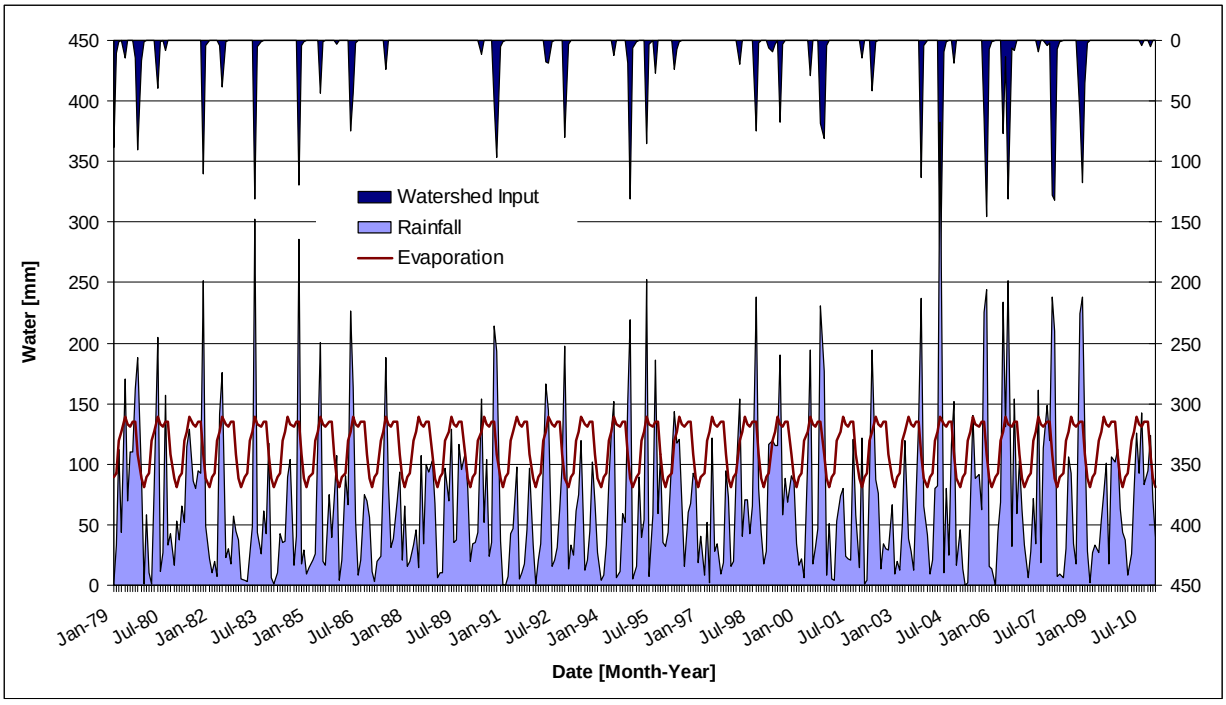

Figure 14. Simulated and Measured Water Balance Variables for the Lake Saumatre Watershed from 1979 to 2010.

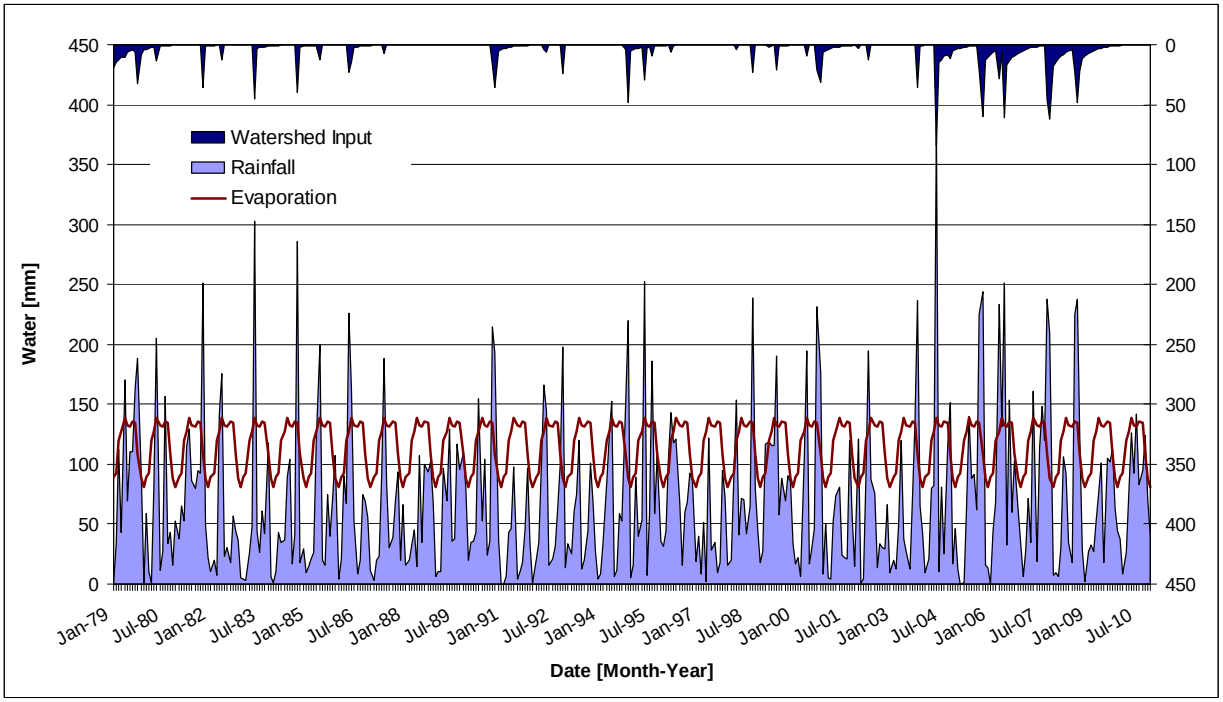

Figure 15. Simulated and Measured Water Balance Variables for the Lake Enriquillo Watershed from 1979 to 2010.

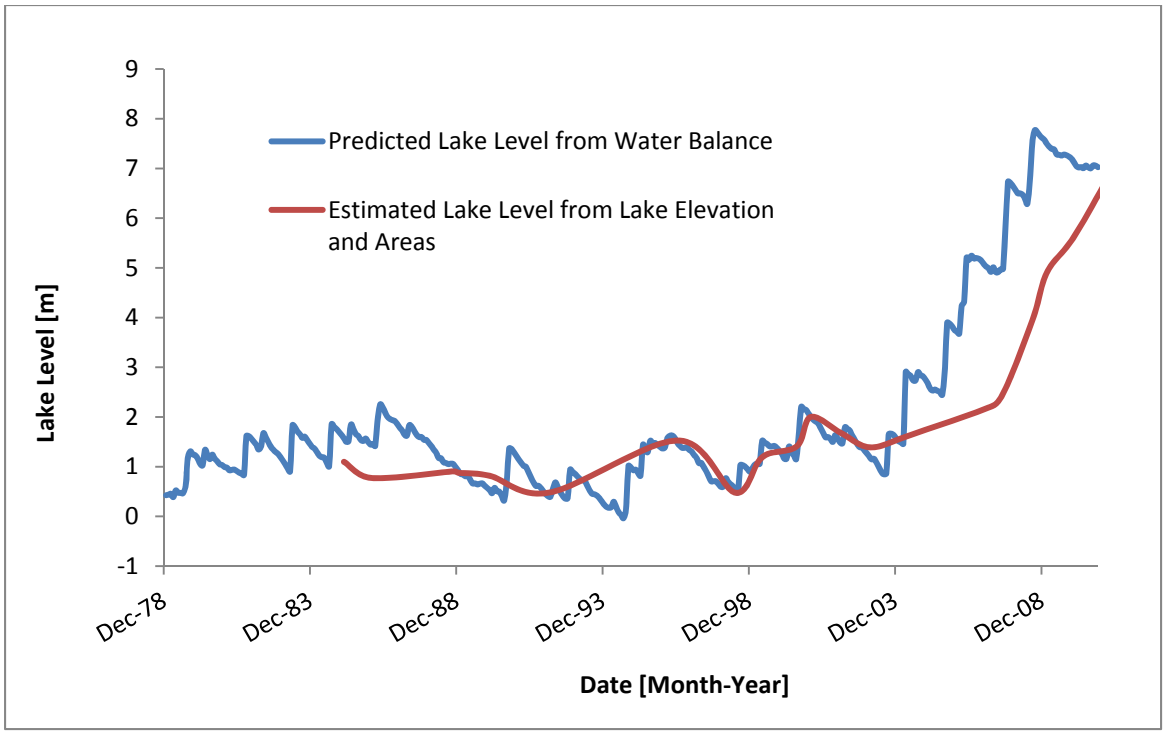

Figure 16. Simulated and Measured Lake Elevation for Lake Saumatre from 1979 to 2010.

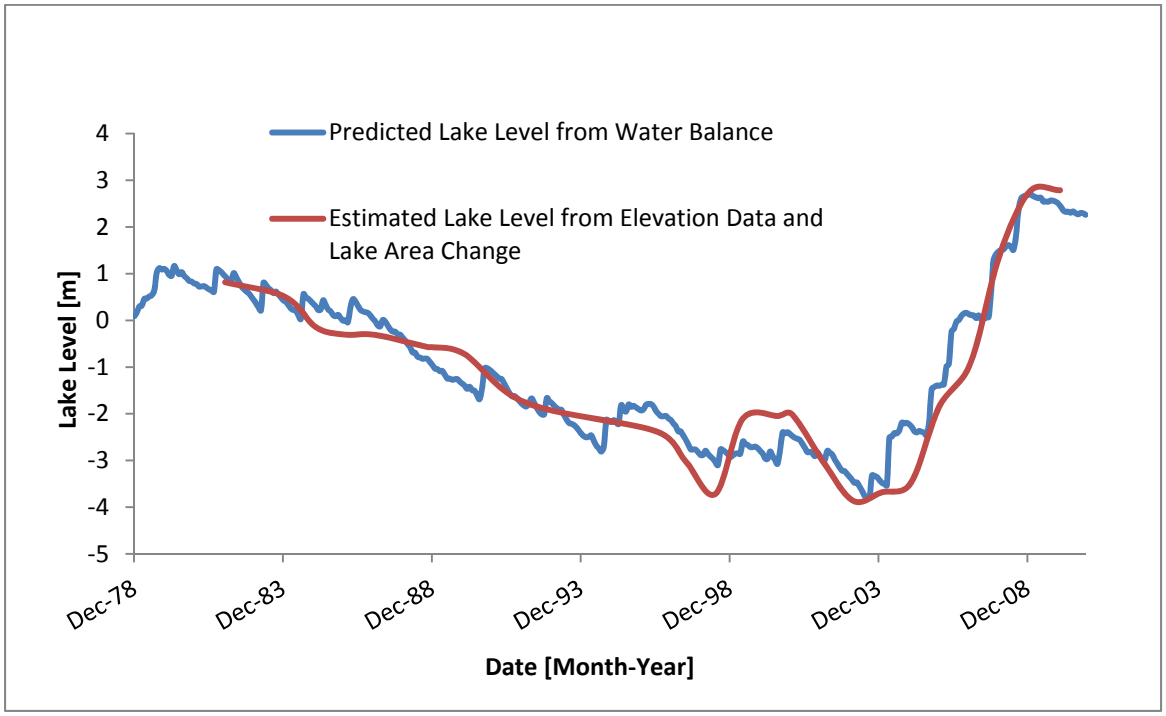

Figure 17. Simulated and Measured Lake Elevation for Lake Enriquillo from 1979 to 2010.

4. Discussion and Conclusions

The results obtained in the study mainly demonstrate that fluctuations in precipitation could potentially account for the major changes in lakes' levels over the time period of interest. The lakes' levels closely correlate to precipitation patterns. Although the watershed area is severely deforested, minimal changes in land use and land cover indicate that changing forest cover cannot be a significant factor in the lake's behavior. The lakes are highly sensitive to rainfall and evaporative changes in the watershed. The water rise in the lakes is likely due to a greater number of high precipitation events during the last few years exceeding soil capacity.

It is hoped that this study sets the stage for further research into the dynamics of these watersheds. If precipitation patterns remain the same as well as other climatic parameters, then the lakes will probably continue increasing in size, further damaging goods, lands and structures. Further research needs to be done to understand the dynamics of these zones and to prepare contingency plans in case the lakes do keep increasing in size, whether the plans are to evacuate the people that live around the area or draining the lake by means of canals.

5. Bibliography

Buck, D. G., Brenner, M., Hodell, D. A., Curits, J. H., Martin, J. B., &Pagani, M. (2005). Physical and chemical properties of hypersalinelagoenriquillo, dominican republic.*Verhandlungen Internationale Vereinigung Für Theoretische Und Angewandte Limnologie, 29*

The caribbean's biggest lake gets bigger, drowns farms. (2010, September 14). *Dominican Today.*

Growing lake swallows main Dominican-Haiti border pass. (2010, June 11). *DominicanToday.*

Cocco Quezada, Antonio (2009). El Ciclo Hidrológico del Lago Enriquillo y la Crecida Extrema del 2009. <http://www.acqweather.com/EL%20CICLO%20HIDROLOGICO%20DEL%20LAGO%20ENRIQUILLO.pdf.>

Kalff, J. (2002). *Limnology* Prentice-Hall, Inc.

Lewis, L. A., & Coffey, W. J. (1985). The continuing deforestation of haiti.*Ambio, 14*(3), pp. 158-160.

Lyzenga, D. R. (1978).Passive remote sensing techniques for mapping water depth and bottom features.*AppliedOptics, 17*(8)

Pierre, M. G. P. A., Molière, E., Amilcar, H., Baptiste, S., D. J, & Robert, G. (2008). *Point de vue de l'Université quisqueya (UniQ) et de l'Ecole nationale de géologie appliquée (ENGA) relatif à la remontée du lac azuei ou étang saumâtre et de l'étang de miragoâne.* Port-au-Prince: l'Université Quisqueya (UniQ) and de l'Ecole Nationale de Géologie Appliquée (ENGA).

Pimentel, Hillman. "Indrhi Dice Deforestación Afecta El Lago Enriquillo." *Periodico El Dia*. El Dia, 13 June 2011. Web. 24 July 2011. <http://www.eldia.com.do/nacionales/2011/6/13/55037/Indrhi-dice-deforestacion-afecta-el-lago-Enriquillo>. Pimentel, Hillman. "Indrhi Dice Deforestación Afecta El Lago Enriquillo." *Periodico El Dia*. El Dia, 13 June 2011. Web. 24 July 2011. <http://www.eldia.com.do/nacionales/2011/6/13/55037/Indrhi-dice-deforestacion-afecta-el-lago-Enriquillo>.

Richards, J. A., and XiupingJia. *Remote Sensing Digital Image Analysis: an Introduction*. Berlin: Springer, 2006. Print.

Steenhuis, T. S., &Molen, W. H. (1896).The thorhthwaite-mather procedure as a simple engineering method to predict recharge.*Journal of Hydrology, 84*, 221.

Stumpf, R. P., Holderied, K., & Sinclair, M. (2003).Determination of water depth with high-resolution satellite imagery over variable bottom types. *Limnology and Oceanography, 48*(1, Part 2; Light in Shallow Waters), pp. 547-556.

Thornthwaite, C. W., & Mather, J. R. (1957). Instructions and tables for computing potential evapotranspiration and the water balance. *Publications in Climatology, 10*(3)

US Army Corps of Engineers (USACE).(1999). *Water resources assessment of Haiti.*

Vlaminck, B. (1989). *La pecherie de l'etangsaumatre: Recherche appliquee et activitesperiode octobre 88-septembre 89.*No. HAI/88/003).United Nations Development Programme/Food and Agriculture Organization (PNUD/FAO). Retrieved from http://www.fao.org/docrep/field/003/AC561F/AC561F00.htm#TOC

William, M. (2011). *Exploration des cause de la montee des eaux de l'etangsaumatre.*Retrieved, 2011, from http://www.jsf-post.com/tag/etang-saumatre/

Yimer, F., Messing, I., Ledin, S. and Abdelkadir, A. (2008), Effects of different land use types on infiltration capacity in a catchment in the highlands of Ethiopia. Soil Use and Management, 24: 344–349. doi: 10.1111/j.1475-2743.2008.00182.

6. Appendix

6.1 Lake-Surface Area Time Series

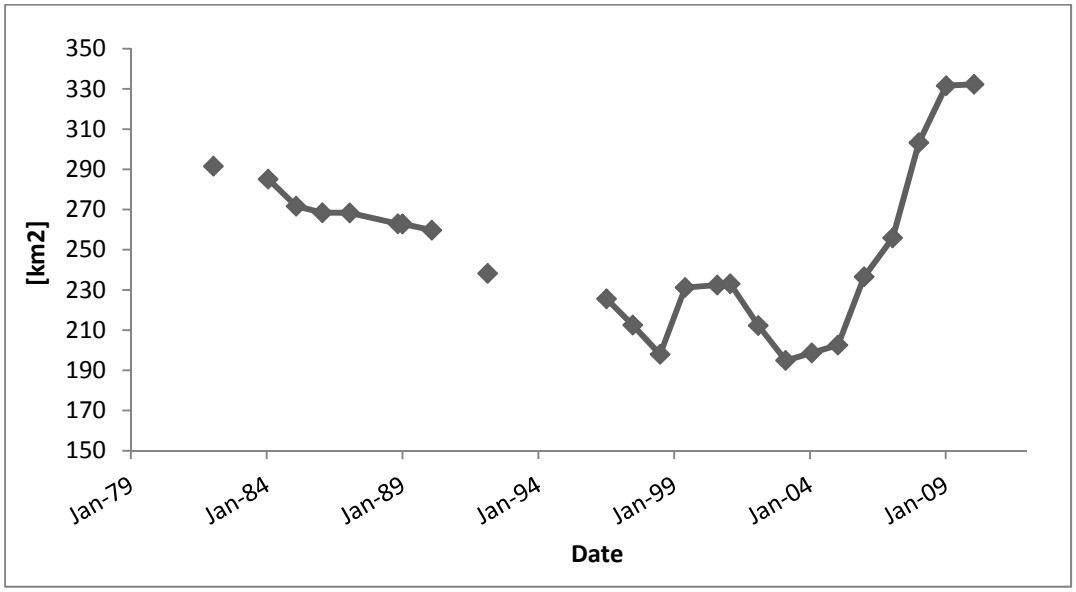

Figure 18. Lake Area Time Series of Lake Enriquillo.

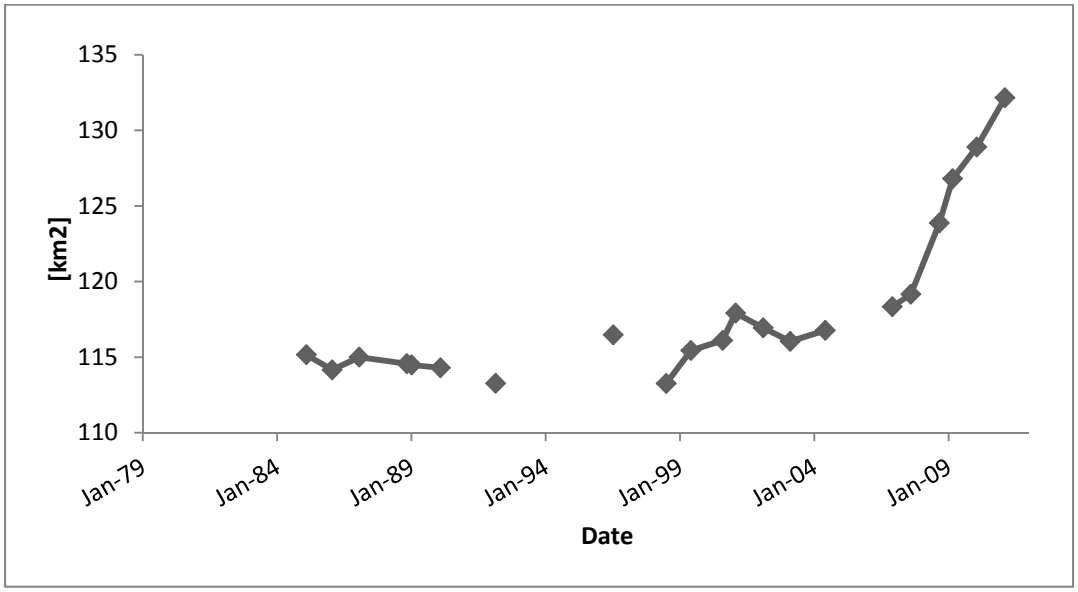

Figure 19. Lake Area Time Series of Lake Saumatre.

6.2. Water Quality Values for Lake Saumatre

Characteristics	Sources	LakeSaumatre
1. Conductivity (micro ohm/cm)	430–500	12000–15500
2. Total Hardness (mg/l)	190–239	1100–2260
3. Total Alkalinity (mg/l)	229–247	194–247
4. Total Cations (mg/l)	84–110	1303–3727
5. Total Anions (mg/l)	251–443	3289–6555
6. pH	7.1–7.8	7.5–8.1
7. Salinity (PPT)	0	7–15
8. Visibility (cm)	-	2.0–3.2
9. Temperature (°C)	22.5–25.5	27–30.5

(Vlaminck, 1989)

6.3. Values for Monthly Water Balance. Monthly rainfall data from Damien station was obtained from the Ministry of Agriculture, Natural Resources and Rural Development (MARDNR) in Haiti and the Jimani station data was obtained from the Department of Climatology in the Dominican Republic.

Date	Rainfall - Jimani	Rainfall Saumatre Thiessen	Long Term Evaporation	Lake Level Estimate-Saumatre	Lake Level Estimate Enriquilo
Month-Year	[m]	[m]	[m]	[m]	[m]
Jan-79	0.00	0.00	0.09	0.42	0.09
Feb-79	0.03	0.03	0.09	0.43	0.18
Mar-79	0.12	0.11	0.12	0.45	0.30
Apr-79	0.02	0.04	0.13	0.38	0.32
May-79	0.17	0.17	0.14	0.49	0.46
Jun-79	0.06	0.07	0.13	0.44	0.47
Jul-79	0.12	0.11	0.13	0.44	0.51
Aug-79	0.10	0.11	0.14	0.43	0.54
Sep-79	0.17	0.16	0.13	0.53	0.64
Oct-79	0.17	0.19	0.11	1.09	1.03
Nov-79	0.10	0.09	0.09	1.18	1.12
Dec-79	0.00	0.00	0.08	1.12	1.09
Jan-80	0.07	0.06	0.09	1.10	1.10
Feb-80	0.00	0.01	0.09	1.02	1.06
Mar-80	0.00	0.00	0.12	0.92	0.97
Apr-80	0.06	0.08	0.13	0.88	0.96
May-80	0.23	0.20	0.14	1.17	1.16
Jun-80	0.00	0.01	0.13	1.06	1.07
Jul-80	0.02	0.03	0.13	0.97	0.99
Aug-80	0.18	0.16	0.14	1.05	1.03
Sep-80	0.02	0.03	0.13	0.96	0.95
Oct-80	0.02	0.04	0.11	0.91	0.90
Nov-80	0.01	0.02	0.09	0.84	0.85
Dec-80	0.04	0.05	0.08	0.82	0.83
Jan-81	0.02	0.04	0.09	0.78	0.79
Feb-81	0.07	0.07	0.09	0.76	0.78
Mar-81	0.06	0.05	0.12	0.71	0.72
Apr-81	0.10	0.11	0.13	0.71	0.73
May-81	0.10	0.13	0.14	0.72	0.73
Jun-81	0.08	0.09	0.13	0.68	0.70
Jul-81	0.07	0.08	0.13	0.65	0.67
Aug-81	0.09	0.09	0.14	0.62	0.64
Sep-81	0.10	0.09	0.13	0.59	0.61
Oct-81	0.22	0.25	0.11	1.35	1.09
Nov-81	0.04	0.05	0.09	1.34	1.07
Dec-81	0.01	0.02	0.08	1.29	1.03
Jan-82	0.00	0.01	0.09	1.22	0.97
Feb-82	0.02	0.02	0.09	1.16	0.91
Mar-82	0.01	0.01	0.12	1.06	0.82
Apr-82	0.13	0.14	0.13	1.10	0.85
May-82	0.19	0.18	0.14	1.34	1.01
Jun-82	0.01	0.02	0.13	1.24	0.92
Jul-82	0.03	0.03	0.13	1.16	0.84
Aug-82	0.01	0.02	0.14	1.05	0.73
Sep-82	0.05	0.06	0.13	0.99	0.67
Oct-82	0.02	0.04	0.11	0.94	0.62
Nov-82	0.03	0.04	0.09	0.90	0.58
Dec-82	0.00	0.01	0.08	0.83	0.51
Jan-83	0.00	0.00	0.09	0.76	0.44
Feb-83	0.00	0.00	0.09	0.68	0.36
Mar-83	0.02	0.03	0.12	0.60	0.28
Apr-83	0.05	0.05	0.13	0.53	0.22
May-83	0.30	0.30	0.14	1.43	0.80
Jun-83	0.04	0.04	0.13	1.39	0.76
Jul-83	0.02	0.03	0.13	1.30	0.69
Aug-83	0.04	0.06	0.14	1.24	0.65
Sep-83	0.04	0.04	0.13	1.16	0.58
Oct-83	0.10	0.12	0.11	1.18	0.62
Nov-83	0.00	0.01	0.09	1.11	0.55

Dec-83	0.00	0.00	0.08	1.04	0.49
Jan-84	0.00	0.01	0.09	0.97	0.43
Feb-84	0.04	0.04	0.09	0.93	0.39
Mar-84	0.03	0.04	0.12	0.86	0.33
Apr-84	0.03	0.04	0.13	0.78	0.25
May-84	0.08	0.09	0.14	0.75	0.22
Jun-84	0.10	0.10	0.13	0.73	0.21
Jul-84	0.01	0.02	0.13	0.63	0.11
Aug-84	0.04	0.04	0.14	0.55	0.03
Sep-84	0.29	0.29	0.13	1.37	0.56
Oct-84	0.00	0.02	0.11	1.32	0.50
Nov-84	0.02	0.03	0.09	1.27	0.46
Dec-84	0.00	0.01	0.08	1.21	0.41
Jan-85	0.00	0.01	0.09	1.15	0.35
Feb-85	0.02	0.02	0.09	1.08	0.30
Mar-85	0.01	0.03	0.12	1.00	0.22
Apr-85	0.12	0.12	0.13	1.01	0.23
May-85	0.23	0.20	0.14	1.29	0.43
Jun-85	0.02	0.02	0.13	1.20	0.33
Jul-85	0.01	0.02	0.13	1.10	0.24
Aug-85	0.06	0.07	0.14	1.05	0.19
Sep-85	0.03	0.04	0.13	0.97	0.11
Oct-85	0.08	0.07	0.11	0.94	0.09
Nov-85	0.11	0.11	0.09	0.98	0.12
Dec-85	0.00	0.00	0.08	0.91	0.05
Jan-86	0.01	0.02	0.09	0.86	-0.01
Feb-86	0.09	0.09	0.09	0.86	0.00
Mar-86	0.06	0.07	0.12	0.82	-0.04
Apr-86	0.23	0.23	0.13	1.33	0.28
May-86	0.18	0.16	0.14	1.59	0.45
Jun-86	0.06	0.05	0.13	1.54	0.41
Jul-86	0.00	0.01	0.13	1.43	0.31
Aug-86	0.01	0.02	0.14	1.33	0.23
Sep-86	0.09	0.07	0.13	1.29	0.19
Oct-86	0.05	0.07	0.11	1.26	0.17
Nov-86	0.04	0.06	0.09	1.24	0.16
Dec-86	0.00	0.01	0.08	1.18	0.10
Jan-87	0.00	0.00	0.09	1.10	0.03
Feb-87	0.02	0.02	0.09	1.04	-0.03
Mar-87	0.02	0.02	0.12	0.96	-0.11
Apr-87	0.07	0.09	0.13	0.93	-0.13
May-87	0.17	0.19	0.14	1.12	0.01
Jun-87	0.08	0.08	0.13	1.09	-0.03
Jul-87	0.01	0.03	0.13	1.00	-0.11
Aug-87	0.04	0.04	0.14	0.92	-0.19
Sep-87	0.05	0.07	0.13	0.87	-0.24
Oct-87	0.07	0.09	0.11	0.86	-0.24
Nov-87	0.02	0.02	0.09	0.81	-0.30
Dec-87	0.07	0.07	0.08	0.80	-0.31
Jan-88	0.02	0.02	0.09	0.74	-0.37
Feb-88	0.02	0.02	0.09	0.67	-0.43
Mar-88	0.03	0.03	0.12	0.60	-0.51
Apr-88	0.04	0.05	0.13	0.53	-0.57
May-88	0.01	0.01	0.14	0.42	-0.68
Jun-88	0.06	0.11	0.13	0.41	-0.69
Jul-88	0.03	0.03	0.13	0.33	-0.78
Aug-88	0.07	0.10	0.14	0.31	-0.80
Sep-88	0.08	0.09	0.13	0.28	-0.82
Oct-88	0.11	0.10	0.11	0.29	-0.82
Nov-88	0.07	0.07	0.09	0.28	-0.83
Dec-88	0.00	0.01	0.08	0.21	-0.89
Jan-89	0.00	0.01	0.09	0.14	-0.96
Feb-89	0.01	0.01	0.09	0.07	-1.03
Mar-89	0.09	0.10	0.12	0.06	-1.04
Apr-89	0.07	0.07	0.13	0.02	-1.09
May-89	0.12	0.13	0.14	0.02	-1.08
Jun-89	0.04	0.04	0.13	-0.06	-1.17
Jul-89	0.01	0.04	0.13	-0.14	-1.24
Aug-89	0.10	0.12	0.14	-0.14	-1.25
Sep-89	0.08	0.10	0.13	-0.17	-1.27
Oct-89	0.09	0.11	0.11	-0.16	-1.26
Nov-89	0.06	0.08	0.09	-0.15	-1.26
Dec-89	0.01	0.02	0.08	-0.21	-1.31
Jan-90	0.03	0.03	0.09	-0.25	-1.36
Feb-90	0.02	0.04	0.09	-0.30	-1.40
Mar-90	0.02	0.04	0.12	-0.36	-1.47
Apr-90	0.16	0.15	0.13	-0.27	-1.42
May-90	0.04	0.05	0.14	-0.34	-1.49
Jun-90	0.10	0.10	0.13	-0.36	-1.51
Jul-90	0.02	0.02	0.13	-0.45	-1.60
Aug-90	0.03	0.04	0.14	-0.53	-1.69
Sep-90	0.23	0.21	0.13	-0.17	-1.44
Oct-90	0.20	0.19	0.11	0.46	-1.03
Nov-90	0.03	0.04	0.09	0.44	-1.02
Dec-90	0.00	0.00	0.08	0.37	-1.06
Jan-91	0.00	0.00	0.09	0.29	-1.11
Feb-91	0.00	0.01	0.09	0.22	-1.16
Mar-91	0.04	0.04	0.12	0.15	-1.20
Apr-91	0.04	0.05	0.13	0.09	-1.25
May-91	0.09	0.10	0.14	0.06	-1.26
Jun-91	0.00	0.00	0.13	-0.05	-1.36
Jul-91	0.00	0.01	0.13	-0.16	-1.46
Aug-91	0.01	0.02	0.14	-0.26	-1.56
Sep-91	0.01	0.05	0.13	-0.34	-1.62
Oct-91	0.10	0.10	0.11	-0.33	-1.62
Nov-91	0.02	0.03	0.09	-0.38	-1.66
Dec-91	0.00	0.00	0.08	-0.45	-1.73
Jan-92	0.02	0.02	0.09	-0.51	-1.79
Feb-92	0.03	0.03	0.09	-0.56	-1.83
Mar-92	0.09	0.10	0.12	-0.57	-1.84
Apr-92	0.17	0.17	0.13	-0.43	-1.75
May-92	0.15	0.14	0.14	-0.33	-1.67
Jun-92	0.01	0.02	0.13	-0.44	-1.77
Jul-92	0.02	0.02	0.13	-0.53	-1.87
Aug-92	0.03	0.03	0.14	-0.62	-1.96
Sep-92	0.04	0.06	0.13	-0.68	-2.01
Oct-92	0.05	0.10	0.11	-0.67	-2.01
Nov-92	0.20	0.20	0.09	-0.13	-1.67
Dec-92	0.01	0.01	0.08	-0.18	-1.73
Jan-93	0.03	0.03	0.09	-0.22	-1.77

Feb-93	0.02	0.03	0.09	-0.28	-1.83
Mar-93	0.06	0.06	0.12	-0.33	-1.88
Apr-93	0.06	0.07	0.13	-0.37	-1.91
May-93	0.11	0.12	0.14	-0.37	-1.92
Jun-93	0.01	0.01	0.13	-0.47	-2.02
Jul-93	0.02	0.02	0.13	-0.57	-2.12
Aug-93	0.03	0.04	0.14	-0.65	-2.20
Sep-93	0.07	0.10	0.13	-0.67	-2.22
Oct-93	0.06	0.07	0.11	-0.69	-2.24
Nov-93	0.01	0.03	0.09	-0.75	-2.29
Dec-93	0.00	0.00	0.08	-0.81	-2.36
Jan-94	0.00	0.01	0.09	-0.88	-2.43
Feb-94	0.04	0.03	0.09	-0.93	-2.48
Mar-94	0.07	0.08	0.12	-0.96	-2.50
Apr-94	0.11	0.13	0.13	-0.94	-2.49
May-94	0.14	0.15	0.14	-0.87	-2.46
Jun-94	0.00	0.01	0.13	-0.98	-2.57
Jul-94	0.00	0.01	0.13	-1.08	-2.68
Aug-94	0.04	0.06	0.14	-1.14	-2.74
Sep-94	0.04	0.05	0.13	-1.21	-2.81
Oct-94	0.15	0.15	0.11	-1.06	-2.71
Nov-94	0.22	0.22	0.09	-0.20	-2.13
Dec-94	0.00	0.01	0.08	-0.23	-2.15
Jan-95	0.00	0.02	0.09	-0.29	-2.18
Feb-95	0.08	0.09	0.09	-0.29	-2.14
Mar-95	0.03	0.04	0.12	-0.35	-2.18
Apr-95	0.05	0.05	0.13	-0.41	-2.22
May-95	0.27	0.25	0.14	0.18	-1.82
Jun-95	0.01	0.01	0.13	0.08	-1.91
Jul-95	0.05	0.06	0.13	0.03	-1.95
Aug-95	0.17	0.19	0.14	0.22	-1.80
Sep-95	0.07	0.06	0.13	0.16	-1.85
Oct-95	0.12	0.11	0.11	0.17	-1.83
Nov-95	0.02	0.04	0.09	0.13	-1.87
Dec-95	0.03	0.03	0.08	0.09	-1.90
Jan-96	0.04	0.04	0.09	0.05	-1.93
Feb-96	0.07	0.10	0.09	0.07	-1.90
Mar-96	0.15	0.14	0.12	0.22	-1.81
Apr-96	0.11	0.12	0.13	0.23	-1.79
May-96	0.11	0.12	0.14	0.23	-1.79
Jun-96	0.06	0.07	0.13	0.18	-1.84
Jul-96	0.01	0.02	0.13	0.08	-1.94
Aug-96	0.03	0.06	0.14	0.02	-2.00
Sep-96	0.06	0.07	0.13	-0.03	-2.05
Oct-96	0.08	0.09	0.11	-0.04	-2.05
Nov-96	0.08	0.09	0.09	-0.03	-2.05
Dec-96	0.01	0.02	0.08	-0.08	-2.10
Jan-97	0.03	0.04	0.09	-0.12	-2.14
Feb-97	0.00	0.01	0.09	-0.20	-2.21
Mar-97	0.05	0.05	0.12	-0.25	-2.26
Apr-97	0.00	0.00	0.13	-0.36	-2.38
May-97	0.11	0.12	0.14	-0.36	-2.38
Jun-97	0.02	0.03	0.13	-0.45	-2.47
Jul-97	0.03	0.03	0.13	-0.54	-2.55
Aug-97	0.00	0.01	0.14	-0.65	-2.66
Sep-97	0.01	0.02	0.13	-0.75	-2.76
Oct-97	0.05	0.09	0.11	-0.75	-2.76
Nov-97	0.02	0.07	0.09	-0.76	-2.77
Dec-97	0.02	0.02	0.08	-0.81	-2.82
Jan-98	0.02	0.02	0.09	-0.87	-2.88
Feb-98	0.07	0.09	0.09	-0.86	-2.88
Mar-98	0.17	0.15	0.12	-0.72	-2.79
Apr-98	0.03	0.04	0.13	-0.80	-2.86
May-98	0.07	0.07	0.14	-0.85	-2.92
Jun-98	0.05	0.07	0.13	-0.90	-2.96
Jul-98	0.03	0.04	0.13	-0.97	-3.04
Aug-98	0.05	0.07	0.14	-1.03	-3.09
Sep-98	0.23	0.24	0.13	-0.51	-2.76
Oct-98	0.09	0.08	0.11	-0.51	-2.78
Nov-98	0.02	0.04	0.09	-0.55	-2.82
Dec-98	0.00	0.02	0.08	-0.60	-2.87
Jan-99	0.02	0.03	0.09	-0.65	-2.92
Feb-99	0.11	0.12	0.09	-0.59	-2.89
Mar-99	0.08	0.12	0.12	-0.54	-2.85
Apr-99	0.13	0.12	0.13	-0.53	-2.85
May-99	0.11	0.12	0.14	-0.54	-2.85
Jun-99	0.20	0.19	0.13	-0.14	-2.60
Jul-99	0.04	0.06	0.13	-0.19	-2.64
Aug-99	0.07	0.09	0.14	-0.22	-2.67
Sep-99	0.05	0.07	0.13	-0.27	-2.71
Oct-99	0.10	0.09	0.11	-0.28	-2.71
Nov-99	0.09	0.09	0.09	-0.27	-2.70
Dec-99	0.03	0.03	0.08	-0.31	-2.74
Jan-00	0.02	0.02	0.09	-0.37	-2.80
Feb-00	0.00	0.02	0.09	-0.43	-2.86
Mar-00	0.00	0.01	0.12	-0.53	-2.95
Apr-00	0.09	0.10	0.13	-0.54	-2.96
May-00	0.17	0.19	0.14	-0.33	-2.81
Jun-00	0.01	0.02	0.13	-0.43	-2.91
Jul-00	0.01	0.03	0.13	-0.51	-2.99
Aug-00	0.04	0.05	0.14	-0.59	-3.07
Sep-00	0.25	0.23	0.13	-0.11	-2.76
Oct-00	0.18	0.18	0.11	0.41	-2.40
Nov-00	0.01	0.01	0.09	0.36	-2.42
Dec-00	0.06	0.05	0.08	0.34	-2.40
Jan-01	0.01	0.00	0.09	0.27	-2.43
Feb-01	0.00	0.00	0.09	0.19	-2.48
Mar-01	0.05	0.05	0.12	0.14	-2.51
Apr-01	0.04	0.07	0.13	0.10	-2.54
May-01	0.06	0.08	0.14	0.05	-2.56
Jun-01	0.02	0.02	0.13	-0.04	-2.64
Jul-01	0.02	0.02	0.13	-0.13	-2.73
Aug-01	0.00	0.02	0.14	-0.23	-2.82
Sep-01	0.12	0.12	0.13	-0.23	-2.81
Oct-01	0.04	0.06	0.11	-0.27	-2.85
Nov-01	0.01	0.01	0.09	-0.34	-2.91
Dec-01	0.13	0.12	0.08	-0.21	-2.83
Jan-02	0.00	0.00	0.09	-0.29	-2.90
Feb-02	0.00	0.00	0.09	-0.37	-2.98
Mar-02	0.08	0.09	0.12	-0.38	-2.99

Apr-02	0.15	0.19	0.13	-0.09	-2.80
May-02	0.09	0.09	0.14	-0.12	-2.83
Jun-02	0.09	0.08	0.13	-0.16	-2.87
Jul-02	0.01	0.01	0.13	-0.27	-2.98
Aug-02	0.02	0.03	0.14	-0.35	-3.06
Sep-02	0.02	0.03	0.13	-0.44	-3.15
Oct-02	0.01	0.03	0.11	-0.51	-3.22
Nov-02	0.04	0.07	0.09	-0.52	-3.23
Dec-02	0.01	0.01	0.08	-0.59	-3.29
Jan-03	0.02	0.02	0.09	-0.65	-3.35
Feb-03	0.01	0.01	0.09	-0.72	-3.42
Mar-03	0.03	0.05	0.12	-0.77	-3.48
Apr-03	0.12	0.12	0.13	-0.77	-3.47
May-03	0.03	0.04	0.14	-0.85	-3.56
Jun-03	0.01	0.03	0.13	-0.94	-3.65
Jul-03	0.01	0.01	0.13	-1.05	-3.75
Aug-03	0.05	0.07	0.14	-1.09	-3.80
Sep-03	0.11	0.14	0.13	-1.08	-3.78
Oct-03	0.17	0.24	0.11	-0.34	-3.32
Nov-03	0.07	0.07	0.09	-0.33	-3.33
Dec-03	0.05	0.04	0.08	-0.36	-3.35
Jan-04	0.01	0.01	0.09	-0.43	-3.42
Feb-04	0.01	0.02	0.09	-0.49	-3.48
Mar-04	0.08	0.08	0.12	-0.51	-3.50
Apr-04	0.07	0.08	0.13	-0.54	-3.53
May-04	0.31	0.38	0.14	0.87	-2.52
Jun-04	0.01	0.01	0.13	0.81	-2.49
Jul-04	0.08	0.08	0.13	0.78	-2.41
Aug-04	0.01	0.03	0.14	0.69	-2.42
Sep-04	0.13	0.12	0.13	0.68	-2.35
Oct-04	0.16	0.15	0.11	0.84	-2.19
Nov-04		0.02	0.09	0.77	-2.21
Dec-04		0.05	0.08	0.75	-2.19
Jan-05	0.00	0.01	0.09	0.68	-2.23
Feb-05	0.00	0.00	0.09	0.60	-2.28
Mar-05	0.00	0.00	0.12	0.49	-2.37
Apr-05	0.05	0.07	0.13	0.45	-2.40
May-05	0.13	0.14	0.14	0.46	-2.37
Jun-05	0.08	0.09	0.13	0.43	-2.39
Jul-05	0.11	0.09	0.13	0.41	-2.40
Aug-05	0.04	0.06	0.14	0.35	-2.45
Sep-05	0.24	0.23	0.13	0.79	-2.16
Oct-05	0.26	0.24	0.11	1.74	-1.48
Nov-05	0.00	0.02	0.09	1.72	-1.43
Dec-05	0.02	0.01	0.08	1.67	-1.40
Jan-06	0.00	0.00	0.09	1.59	-1.40
Feb-06	0.05	0.04	0.09	1.55	-1.38
Mar-06	0.05	0.07	0.12	1.51	-1.37
Apr-06	0.17	0.23	0.13	2.04	-0.99
May-06	0.10	0.13	0.14	2.10	-0.93
Jun-06	0.20	0.25	0.13	2.96	-0.25
Jul-06	0.01	0.03	0.13	2.91	-0.18
Aug-06	0.15	0.15	0.14	2.97	-0.03
Sep-06	0.06	0.06	0.13	2.91	0.01
Oct-06	0.10	0.10	0.11	2.92	0.10
Nov-06	0.07	0.06	0.09	2.90	0.15
Dec-06	0.00	0.03	0.08	2.87	0.16
Jan-07	0.00	0.01	0.09	2.79	0.13
Feb-07	0.00	0.03	0.09	2.74	0.11
Mar-07	0.06	0.07	0.12	2.70	0.11
Apr-07	0.01	0.03	0.13	2.62	0.05
May-07	0.15	0.16	0.14	2.70	0.11
Jun-07	0.02	0.02	0.13	2.60	0.02
Jul-07	0.10	0.11	0.13	2.60	0.03
Aug-07	0.16	0.15	0.14	2.63	0.07
Sep-07	0.12	0.12	0.13	2.63	0.08
Oct-07	0.23	0.24	0.11	3.45	0.63
Nov-07	0.23	0.21	0.09	4.31	1.31
Dec-07	0.01	0.01	0.08	4.29	1.41
Jan-08	0.00	0.01	0.09	4.22	1.48
Feb-08	0.00	0.01	0.09	4.15	1.51
Mar-08	0.02	0.03	0.12	4.07	1.52
Apr-08	0.09	0.11	0.13	4.06	1.58
May-08	0.06	0.09	0.14	4.03	1.61
Jun-08	0.02	0.03	0.13	3.95	1.57
Jul-08	0.01	0.02	0.13	3.85	1.51
Aug-08	0.21	0.22	0.14	4.28	1.82
Sep-08	0.18	0.24	0.13	5.04	2.37
Oct-08	0.12	0.12	0.11	5.24	2.60
Nov-08	0.03	0.03	0.09	5.20	2.66
Dec-08	0.00	0.00	0.08	5.14	2.67
Jan-09	0.03	0.03	0.09	5.08	2.69
Feb-09	0.04	0.03	0.09	5.04	2.69
Mar-09	0.01	0.03	0.12	4.96	2.66
Apr-09	0.06	0.05	0.13	4.90	2.64
May-09	0.08	0.08	0.14	4.85	2.62
Jun-09	0.08	0.10	0.13	4.83	2.62
Jul-09	0.02	0.02	0.13	4.73	2.55
Aug-09	0.11	0.11	0.14	4.72	2.55
Sep-09	0.09	0.10	0.13	4.70	2.54
Oct-09	0.08	0.11	0.11	4.71	2.57
Nov-09	0.05	0.06	0.09	4.70	2.56
Dec-09	0.04	0.04	0.08	4.67	2.54
Jan-10	0.04	0.04	0.09	4.63	2.50
Feb-10	0.00	0.01	0.09	4.56	2.43
Mar-10	0.02	0.03	0.12	4.48	2.36
Apr-10	0.04	0.08	0.13	4.44	2.32
May-10	0.10	0.13	0.14	4.44	2.33
Jun-10	0.09	0.09	0.13	4.42	2.30
Jul-10	0.15	0.14	0.13	4.44	2.33
Aug-10	0.07	0.08	0.14	4.41	2.30
Sep-10	0.08	0.09	0.13	4.38	2.27
Oct-10	0.11	0.12	0.11	4.42	2.30
Nov-10	0.06	0.07	0.09	4.42	2.29
Dec-10	0.03	0.04	0.08	4.38	2.26

6.4. Soil Survey Sites

Site	Elevation	Soil	Erosion	Depth [cm]	H20 [cm/cm]	Longitude	Latitude
St. George	low	basaltic	severe	90	0.07	-73.00	18.25
Bergeau	low	limestone based, calcerous	severe	>22, 40	0.17, 0.18	-73.00	18.21
Fort Jacques	mid-high	limestone		125	0.22	-72.25	18.48
Salagnac	mid-high	limestone	slight	>100		-73.23	18.41
Titanyen	low	limestone, colluvium	slight	40	0.16	-73.00	18.68

Data from Guthrie and Shannon, 2004.